Article

JOURNAL OF COMPOSITE MATERIALS

Journal of Composite Materials
2022, Vol. 56(21) 3269–3293

DOI: 10.1177/00219983221107257
journals.sagepub.com/home/jcm
SAGE

Static and dynamic deformation response of smart laminated composite plates induced by inclined piezoelectric actuators

Soheil Gohari[1], Farzin Mozafari[2], Navid Moslemi[3], Saeed Mouloodi[1], Reza Alebrahim[4], Mizan Ahmed[5,6], Behzad Abdi[7], Izman Sudin[3] and Colin Burvill[1]

Abstract

A Levi-type analytical solution procedure is developed to characterize static and dynamic deformation response of smart laminated simply-supported composite rectangular plates induced by inclined piezoelectric actuators under (1) constant electrical voltage and (2) time-dependent electrical voltage with excitation frequency. The key to development of this analytical solution is to employ higher order finite integral transform and discretized higher order partial differential unit step function equations. Unlike earlier studies, this research aims to investigate the effect of inclination angle of piezoelectric actuators on static and dynamic deformation response of laminated composite plates under both static and dynamic conditions. The developed analytical solution procedure is implemented computationally through Matlab-based computer code. Its accuracy is initially investigated through convergence study and results comparison with the published literature for a particular case when inclination angle is $\theta = 0°$, which is only limited to bending deformation response. Since there is no published benchmark data for twisting deformation response analysis caused by inclination angle of piezoelectric actuators ($\theta \neq 0°$), a set of robust and realistic numerical analysis using Abaqus finite element analysis (FEA) is conducted. Good agreement between the analytical and numerical results is observed. Unlike applied electrical voltage, inclination angle of a piezoelectric actuator does not have a significant impact on twisting deformation response during static mode; whereas, both the excitation frequency and inclination angle can significantly influence maximum amplitude of vibration.

Keywords

twisting response, static and dynamic deformation, inclination angle, piezoelectric actuator, smart laminated composite plate

Introduction

Smart structures integrated with piezoelectric materials and laminated composite plates have attracted much attention in recent decades. These structures combine the outstanding mechanical characteristics of laminated composite materials with the intrinsic capability of piezoelectric materials to sense and tune static and dynamic response of structures.[1–5] Of particular importance in this context is the mechanical analysis of such smart structures under various loads and boundary conditions.

There have been numerous studies that attempted to characterize the mechanical response of smart structures made of orthotropic composite plates integrated with piezoelectric materials.[6–8] In recent decades, three main approaches have been employed to study static and dynamic response of laminated piezoelectric composite plates including: experimental, numerical, and analytical approaches. From an experimental perspective, most of the studies have been conducted in determining the

[1]Department of Mechanical Engineering, The University of Melbourne, Parkville, VIC, AU
[2]Department of Mechanical Engineering, Bilkent University, Ankara, Turkey
[3]School of Mechanical Engineering, Universiti Teknologi Malaysia (UTM), Skudai, Malaysia
[4]Department of Engineering, Roma Tre University, Rome, Italy
[5]School of Civil and Mechanical Engineering, Curtin University, Bentley, WA, AU
[6]Department of Civil Engineering, Monash University, Clayton, VIC, AU
[7]Department of Mechanical, Aerospace and Civil Engineering, The University of Manchester, Manchester, UK

Corresponding author:
Soheil Gohari, Department of Mechanical Engineering, The University of Melbourne, Grattan Street, Parkville, VIC 3010, AU.
Email: soheil.gohari@unimelb.edu.au, soheil.gohari7@gmail.com

vibration characteristics of smart materials. The application of piezoelectric elements embedded in laminated composite structures as an actuator for suppressing the vibration agitation of composite structures has been studied by Yang and Bian.[9] Thinh et al.[10] established an experimental setup to determine static and dynamic behavior of cantilevered piezoelectric composite plates. Furthermore, the experimental results have been used to verify the numerical results obtained from FEA. More recently, Chung et al.[11] investigated the dynamic behavior of smart laminated cantilevered composite plates supplemented by piezoelectric material under the dynamic loading conditions and induced by airflow.

From a numerical standpoint, Lam and coworkers[12] developed an FEA-based methodology to investigate static and vibrational behavior of piezoelectric composite laminates. With the same objective, Balamurugan and Narayanan[13] proposed a FEA model in which shell elements are employed to investigate electromechanical coupling effects of piezoelectric sensor and actuator layers. Recently, In a study conducted by Alimohammadi and Babokani,[14] an FEA-based numerical setting for analyzing the electrostatic and dynamic characteristics of layered piezoelectric composite shells has been developed. However, such attempts, while providing insight into the characterization of the mechanical response of smart structures, have their own shortcomings, which may impose some built-in complexities. Since there are inherent potential sources of modeling and discretization errors in all numerical approaches, special considerations must be given to determine and control such errors.

Therefore, while the numerical approaches are extremely useful to evaluate structural responses of smart structures, the verification of results need extensive quantitative error assessments.[15–18] It is therefore of great interest to develop a reasonable way for predicting the mechanical response of smart structures based upon analytical or so-called exact solution procedures to avoid shortcomings observed in the numerical investigation.

Several studies have been conducted to analytically determine the mechanical response of smart structures, some focusing on dynamic behavior, others on buckling and static behavior. Farsangi and Saidi[19] and Farsangi et al.[20] proposed an analytical solution to describe the free-vibrational features of functionally graded and laminated rectangular plates integrated with piezoelectric layers. In the current work context, Kapuria et al.[21] developed a Levi-type analytical solution to predict bending response of laminated piezoelectric composite plates using the First-Order Shear Deformation Theory. Vel and Batra[22] proposed an exact solution procedure for characterizing bending response of laminated simply-supported plates supplemented by piezoelectric actuator.

Although, further attempts have been made by the researchers[23,24] to establish the analytical solution procedure for describing bending response of smart composite structures, to the best knowledge of authors, there is a lack of studies that deal with the analytical characterization of twisting behavior of laminated piezoelectric composite rectangular plates[25] and this has motivated the present study. The present work's main contribution is the development of a Levi-type analytical solution procedure to describe twisting response of smart laminated simply-supported piezoelectric composite plates. The electro-mechanical twisting coupling in smart simply-supported plates have not, to date, been investigated. In doing so, linear piezoelectricity and Classical Plate Theory (i.e. Kirchhoff Plate Theory) are adopted. Higher order finite integral transform and discretized higher order partial differential unit step function equations, which do not require determination of characteristic functions, are employed to solve partial differential equations associated with the electro-mechanical bending-twisting coupling. The solution procedure, which is applicable to both static and dynamic responses, is implemented computationally through a Matlab-based computer code. To elucidate the present analytical solution's predictive capabilities, the analytical results are initially validated with the published literature for a particular case when inclination angle is $\theta = 0°$. A series of FEA procedures are then conducted to compare with the analytical solution's twisting deformation response.

Analytical solution procedures

This section restricts its attention to developing the analytical approach for characterizing twisting response of smart laminated simply-supported piezoelectric composite plates under static and dynamic stimuli. The mathematical procedures to solve partial differential equations of static equilibrium and motion are discussed.

Static deformation response

In this subsection, an analytical solution for static deformation response of smart laminated simply-supported composite rectangular plates induced by inclined piezoelectric actuators is developed. As shown in Figure 1, Multiple pairs of inclined piezoelectric actuators are bounded to fully characterize twisting response of the smart laminated composite plate with simply-support boundary conditions at all edges.

The governing partial differential equation of static equilibrium associated with a laminated composite

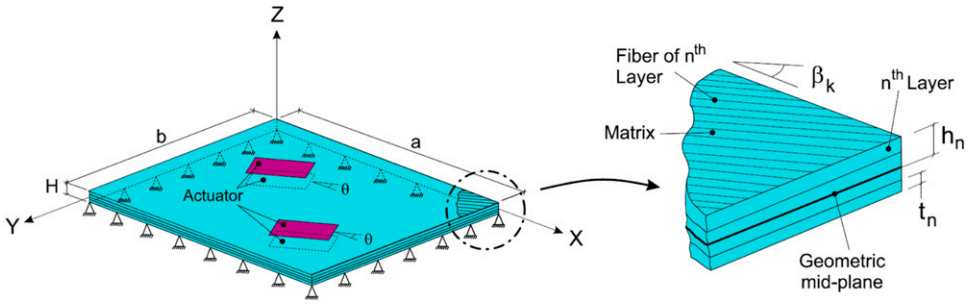

Figure 1. Schematic representation of a host structure (smart laminated simply-supported composite plate) integrated with multiple pairs of inclined piezoelectric actuators. The host structure (composite plate) consists of *N* layers and arbitrary stacking sequence configuration.

rectangular plate induced by inclined piezoelectric actuators is stated in equation (1)[25]

$$D_{11}\frac{\partial^4 w(x,y)}{\partial x^4}+2D_3\frac{\partial^4 w(x,y)}{\partial x^2\partial y^2}+D_{22}\frac{\partial^4 w(x,y)}{\partial y^4}=\sum_{L=1}^{N}P_L^e(x,y,\theta) \tag{1}$$

where, θ is inclination angle between a piezoelectric actuator and the x axis. The expression for bending and twisting couplings known as ${P_L}^e(x, y,\theta)$ is given by equation (2)

$$\sum_{L=1}^{N}P_L^e(x,y,\theta)=\sum_{L=1}^{N}\left(\frac{\partial^2 M_{xx,L}^e(x,y,\theta)}{\partial x^2}+\frac{\partial^2 M_{yy,L}^e(x,y,\theta)}{\partial y^2}+2\frac{\partial^2 M_{xy,L}^e(x,y,\theta)}{\partial x\partial y}\right) \tag{2}$$

where, N stands for the pair number of piezoelectric actuators bonded to the host structure (smart laminated composite plate). ${M_{xx,L}}^e$ and ${M_{yy,L}}^e$ are the electrical bending moments along the x and y axes, respectively, and ${M_{xy,L}}^e$ is the electrical twisting moment, which comes into effect when a piezoelectric actuators has an inclination angle of θ with the x axis. The terms D_{11} and D_{22} in equation (1) are the flexural stiffness, $D_3 = D_{12} + 2D_{66}$ is the effective torsional rigidity, and D_{66} is the torsional rigidity of a laminated composite plate. These coefficients can be given by a general statement in equation (3)

$$D_{ij}=\frac{1}{3}\sum_{K=1}^{N}\sum_{j=1,2,6}\left[\overline{Q}_{ij}\right]_k\left(h_k^3-h_{k-1}^3\right) \tag{3}$$

where, h is the distance of layer k from the rectangular plate's geometric mid-plane (Figure 1). The components of the transformed, reduced stiffness matrix, D_{ij} are determined by the respective relations in equations (4) – (9)

$$\overline{Q}_{11}=Q_{11}c^4+2(Q_{12}+2Q_{66})c^2s^2+Q_{22}s \tag{4}$$

$$\overline{Q}_{12}=(Q_{11}+Q_{22}-4Q_{66})c^2s^2+Q_{12}\left(c^4+s^4\right) \tag{5}$$

$$\overline{Q}_{22}=Q_{11}s^4+2(Q_{12}+2Q_{66})c^2s^2+Q_{22}c^4 \tag{6}$$

$$\overline{Q}_{16}=-Q_{22}cs^3+Q_{11}c^3s-(Q_{12}+2Q_{66})\left(c^2-s^2\right)cs \tag{7}$$

$$\overline{Q}_{26}=-Q_{22}c^3s+Q_{11}cs^3-(Q_{12}+2Q_{66})\left(c^2-s^2\right)cs \tag{8}$$

$$\overline{Q}_{66}=(Q_{11}+Q_{22}-2Q_{12})c^2s^2+Q_{66}\left(c^2-s^2\right)^2 \tag{9}$$

where, c and s stand for the cos(β) and sin(β) and β is the angle between the fiber direction and the x axis in each layer. The quantities Q_{11}, Q_{22}, Q_{12}, and Q_{66} are given by equations (10) – (13), respectively

$$Q_{11}=\frac{E_1}{1-\nu_{12}\nu_{21}} \tag{10}$$

$$Q_{22}=\frac{E_2}{1-\nu_{12}\nu_{21}} \tag{11}$$

$$Q_{12}=\frac{\nu_{12}E_1}{1-\nu_{12}\nu_{21}} \tag{12}$$

$$Q_{66}=G_{12} \tag{13}$$

where, E_{ij}, ν_{ij}, and G_{ij} denote the Young's modulus, Poisson's ratio, and shear modulus in local material ordination, respectively.

To solve the governing partial differential equation of static equilibrium (equation (1)), two boundary conditions need to be prescribed to each edge. In the present study, a simply-supported constraint is imposed at all four edges of the rectangular composite plate as given by equation (14) and equation (15):

$$w(x,y)=0,\ \frac{\partial^2 w}{\partial x^2}=0,\ \ (x=0\ and\ x=a) \tag{14}$$

$$w(x,y)=0,\ \frac{\partial^2 w}{\partial y^2}=0,\ (y=0\ and\ y=b),\qquad \frac{\partial^2 w}{\partial y^2}=0,\ \ (y=0\ and\ y=b) \tag{15}$$

double Fourier series equation associated with the lateral displacements (the displacements along the z axis) in a simply-supported plate is considered as given by equation (16)

$$w(x,y)=\frac{4}{ab}\sum_{m=1,2,3,\ldots}^{\infty}\sum_{n=1,2,3,\ldots}^{\infty} w_{mn}\sin(\alpha_m x)\sin(\beta_n y),\ \left(\alpha_m=\frac{m\pi}{a},\beta_n=\frac{n\pi}{b}\right) \tag{16}$$

where, higher-order Fourier integral transform of equation (16) (i.e. coefficients of double Fourier expansion) is given by equation (17)

$$w_{mn}=\int_0^a\int_0^b w(x,y)\sin(\alpha_m x)\sin(\beta_n y)dxdy,\ (m=1,3,5,\ldots)(n=0,1,2,\ldots) \tag{17}$$

where, a and b denote the length and width of a composite rectangular plate as shown in Figure 1, respectively.

Next, substituting equation (2) into equation (1) and taking higher-order integral transform over both sides of equation (1) as given by equation (18)

$$\begin{aligned}
&D_{11}\int_0^a\int_0^b\frac{\partial^4 w}{\partial x^4}\sin(\alpha_m x)\sin(\beta_n y)dxdy\\
&+2D_3\int_0^a\int_0^b\frac{\partial^4 w}{\partial x^2\partial y^2}\sin(\alpha_m x)\sin(\beta_n y)dxdy\\
&+D_{22}\int_0^a\int_0^b\frac{\partial^4 w}{\partial y^4}\sin(\alpha_m x)\sin(\beta_n y)dxdy\\
&=\int_0^a\int_0^b\sum_{L=1}^{N}\left(\frac{\partial^2 M^e_{xx,L}}{\partial x^2}\right)\sin(\alpha_m x)\sin(\beta_n y)dxdy\\
&+\int_0^a\int_0^b\sum_{L=1}^{N}\left(\frac{\partial^2 M^e_{yy,L}}{\partial y^2}\right)\sin(\alpha_m x)\sin(\beta_n y)dxdy\\
&+2\int_0^a\int_0^b\sum_{L=1}^{N}\left(\frac{\partial^2 M^e_{xy,L}}{\partial x\partial y}\right)\sin(\alpha_m x)\sin(\beta_n y)dxdy
\end{aligned} \tag{18}$$

double finite integral terms of equation (18) yields the expressions in equations (19) – (21). More details of the solution procedure are available in the reference[23] and reference.[25]

$$\begin{aligned}
&\int_0^a\int_0^b\frac{\partial^4 w}{\partial x^4}\sin(\alpha_m x)\sin(\beta_n y)dxdy\\
&=\int_0^b\left[\frac{\partial^3 w}{\partial x^3}\sin(\alpha_m x)\right]_{x=a}\sin(\beta_n y)dy\\
&-\int_0^b\left[\frac{\partial^3 w}{\partial x^3}\sin(\alpha_m x)\right]_{x=0}\sin(\beta_n y)dy\\
&-\alpha_m\int_0^b\left[\frac{\partial^2 w}{\partial x^2}\cos(\alpha_m x)\right]_{x=a}\sin(\beta_n y)dy\\
&+\alpha_m\int_0^b\left[\frac{\partial^2 w}{\partial x^2}\cos(\alpha_m x)\right]_{x=0}\sin(\beta_n y)dy\\
&-\alpha_m^2\int_0^b\left[\frac{\partial w}{\partial x}\sin(\alpha_m x)\right]_{x=a}\sin(\beta_n y)dy\\
&+\alpha_m^2\int_0^b\left[\frac{\partial w}{\partial x}\sin(\alpha_m x)\right]_{x=0}\sin(\beta_n y)dy\\
&+\alpha_m^3\int_0^b\left[w\cos(\alpha_m x)\right]_{x=a}\sin(\beta_n y)dy\\
&-\alpha_m^3\int_0^b\left[w\cos(\alpha_m x)\right]_{x=0}\sin(\beta_n y)dy-\alpha_m^4 w_{mn}
\end{aligned} \tag{19}$$

$$\begin{aligned}
&\int_0^a\int_0^b\frac{\partial^4 w}{\partial x^2\partial y^2}\sin(\alpha_m x)\sin(\beta_n y)dxdy\\
&=\int_0^b\left[\frac{\partial^3 w}{\partial x\partial y^2}\sin(\alpha_m x)\right]_{x=a}\sin(\beta_n y)dy\\
&-\int_0^b\left[\frac{\partial^3 w}{\partial x\partial y^2}\sin(\alpha_m x)\right]_{x=0}\sin(\beta_n y)dy\\
&-\alpha_m\int_0^b\left[\frac{\partial^2 w}{\partial y^2}\cos(\alpha_m x)\right]_{x=a}\sin(\beta_n y)dy\\
&+\alpha_m\int_0^b\left[\frac{\partial^2 w}{\partial y^2}\cos(\alpha_m x)\right]_{x=0}\sin(\beta_n y)dy\\
&-\alpha_m^2\int_0^a\left[\frac{\partial w}{\partial y}\sin(\beta_n y)\right]_{y=b}\sin(\alpha_m x)dx\\
&+\alpha_m^2\int_0^a\left[\frac{\partial w}{\partial y}\sin(\beta_n y)\right]_{y=0}\sin(\alpha_m x)dx\\
&+\alpha_m^2\beta_n\int_0^a\left[w\cos(\beta_n y)\right]_{y=b}\sin(\alpha_m x)dx\\
&-\alpha_m^2\beta_n\int_0^a\left[w\cos(\beta_n y)\right]_{y=0}\sin(\alpha_m x)dx-\alpha_m^2\beta_n^2 w_{mn}
\end{aligned} \tag{20}$$

$$\int_0^a\int_0^b \frac{\partial^4 w}{\partial y^4}\sin(\alpha_m x)\sin(\beta_n y)dxdy = \int_0^a \left[\frac{\partial^3 w}{\partial y^3}\sin(\beta_n y)\right]_{y=b} \sin(\alpha_m x)dx - \int_0^a \left[\frac{\partial^3 w}{\partial y^3}\sin(\beta_n y)\right]_{y=0} \sin(\alpha_m x)dx - \beta_n \int_0^a \left[\frac{\partial^2 w}{\partial y^2}\cos(\beta_n y)\right]_{y=b} \sin(\alpha_m x)dx + \beta_n \int_0^a \left[\frac{\partial^2 w}{\partial y^2}\cos(\beta_n y)\right]_{y=0} \sin(\alpha_m x)dx - \beta_n^2 \int_0^a \left[\frac{\partial w}{\partial y}\sin(\beta_n y)\right]_{y=b} \sin(\alpha_m x)dx + \beta_n^2 \int_0^a \left[\frac{\partial w}{\partial y}\sin(\beta_n y)\right]_{y=0} \sin(\alpha_m x)dx + \beta_n^3 \int_0^a [w\cos(\beta_n y)]_{y=b} \sin(\alpha_m x)dx - \beta_n^3 \int_0^a [w\cos(\beta_n y)]_{y=0} \sin(\alpha_m x)dx - \beta_n^4 w_{mn} \tag{21}$$

To proceed further, equations (19) – (21) are simplified using the associated boundary conditions stated in equation (14) and equation (15).

Solving double finite integral terms of equation (18), containing bending and twisting couplings induced by inclined piezoelectric actuators result in equations (22) – (24)

$$\int_0^a\int_0^b \sum_{L=1}^{N}\left(\frac{\partial^2 M^e_{xx,L}(x,y,\theta)}{\partial x^2}\right)\sin(\alpha_m x)\sin(\beta_n y)dxdy = \int_0^a\int_0^b \sum_{L=1}^{N} M^e_{xx,L}(\theta)\frac{\partial^2}{\partial x^2}\left\{\overline{H_L}(x-x_1)-\overline{H_L}(x-x_2)\right\} \times\left\{\overline{H_L}(y-y_1)-\overline{H_L}(y-y_2)\right\}\sin(\alpha_m x)\sin(\beta_n y)dxdy = \int_0^a\int_0^b \sum_{L=1}^{N} M^e_{xx,L}(\theta)\left\{\delta_L^{'}(x-x_1)-\delta_L^{'}(x-x_2)\right\} \times\left\{\overline{H_L}(y-y_1)-\overline{H_L}(y-y_2)\right\}\sin(\alpha_m x)\sin(\beta_n y)dxdy = \frac{-\beta_n M^e_{xx,L}(\theta)}{\alpha_m}\{\cos(\alpha_m x_{1,L})-\cos(\alpha_m x_{2,L})\} \times\left\{\cos(\beta_n y_{1,L})-\cos(\beta_n y_{2,L})\right\} \tag{22}$$

$$\int_0^a\int_0^b \sum_{L=1}^{N}\left(\frac{\partial^2 M^e_{xy,L}(x,y,\theta)}{\partial x\partial y}\right)\sin(\alpha_m x)\sin(\beta_n y)dxdy = \int_0^a\int_0^b \sum_{L=1}^{N} M^e_{xy,L}(\theta)\frac{\partial^2}{\partial x\partial y}\left\{\overline{H_L}(x-x_1)-\overline{H_L}(x-x_2)\right\} \times\left\{\overline{H_L}(y-y_1)-\overline{H_L}(y-y_2)\right\}\sin(\alpha_m x)\sin(\beta_n y)dxdy = \int_0^a\int_0^b \sum_{L=1}^{N} M^e_{xy,L}(\theta)\{\delta_L(x-x_1)-\delta_L(x-x_2)\} \times\{\delta_L(y-y_1)-\delta_L(y-y_2)\}\sin(\alpha_m x)\sin(\beta_n y)dxdy = M^e_{xy,L}(\theta)\{\sin(\alpha_m x_{1,L})-\sin(\alpha_m x_{2,L})\}\times\{\sin(\beta_n y_{1,L}) - \sin(\beta_n y_{2,L})\} \tag{23}$$

$$\int_0^a\int_0^b \sum_{L=1}^{N}\left(\frac{\partial^2 M^e_{yy,L}(x,y,\theta)}{\partial x^2}\right)\sin(\alpha_m x)\sin(\beta_n y)dxdy = \int_0^a\int_0^b \sum_{L=1}^{N} M^e_{xx,L}(\theta)\frac{\partial^2}{\partial y^2}\left\{\overline{H_L}(x-x_1)-\overline{H_L}(x-x_2)\right\} \times\left\{\overline{H_L}(y-y_1)-\overline{H_L}(y-y_2)\right\}\sin(\alpha_m x)\sin(\beta_n y)dxdy = \int_0^a\int_0^b \sum_{L=1}^{N} M^e_{yy,L}(\theta)\left\{\overline{H_L}(x-x_1)-\overline{H_L}(x-x_2)\right\} \times\{\delta_L^{'}(y-y_1)-\delta_L^{'}(y-y_2)\}\sin(\alpha_m x)\sin(\beta_n y)dxdy = \frac{-\beta_n M^e_{yy,L}(\theta)}{\alpha_m}\{\cos(\alpha_m x_{1,L})-\cos(\alpha_m x_{2,L})\} \times\{\cos(\beta_n y_{1,L})-\cos(\beta_n y_{2,L})\} \tag{24}$$

where, $H(*)$ with bar on top and δ (*) denote the Unit/Heaviside step function and the Dirac delta/Shooting functions of quantity *, respectively. The quantities x_i and y_i with $i = \{1,2\}$ represent the position of piezoelectric actuators. Furthermore, the terms corresponding to bending and twisting coupling can be given by equations (25) – (27)

$$M^e_{xx,L}(\theta) = \frac{1}{2}\sum_{k=1}^{N}\sum_{j=1,2,6}\left[Q_{1j}\right]^k\left[\overline{d}_{3j}(\theta)\right]^k\Psi_{z,L}\left(h_{k+1}^2-h_k^2\right) \tag{25}$$

$$M^e_{yy,L}(\theta) = \frac{1}{2}\sum_{k=1}^{N}\sum_{j=1,2,6}\left[Q_{2j}\right]^k\left[\overline{d}_{3j}(\theta)\right]^k\Psi_{z,L}\left(h_{k+1}^2-h_k^2\right) \tag{26}$$

$$M^{e}_{xy,L}(\theta) = \frac{1}{2}\sum_{k=1}^{N}\sum_{j=1,2,6}\left[Q_{6j}\right]^{k}\left[\overline{d}_{3j}(\theta)\right]^{k}\Psi_{z,L}\left(h^{2}_{k+1} - h^{2}_{k}\right) \tag{27}$$

where,

$$\Psi_{z,L} = \left(\frac{V^{k}}{t^{k}_{pe}}\right)_{L} \tag{28}$$

where, Ψ_z denotes total electrical potential applied to a piezoelectric actuator activated along the z direction and t_{pe} is piezoelectric thickness. The index terms k and L stand for layer and piezoelectric number, respectively. The terms $đ_{31}$, $đ_{32}$, and $đ_{36}$, which are the function of inclination angle θ, are defined in equations (29) – (31), respectively

$$\overline{d}_{31}(\theta) = d_{31}\cos^{2}\theta + d_{32}\sin^{2}\theta \tag{29}$$

$$\overline{d}_{32}(\theta) = d_{31}\sin^{2}\theta + d_{32}\cos^{2}\theta \tag{30}$$

$$\overline{d}_{36}(\theta) = 2(d_{31} - d_{32})\sin\theta\cos\theta \tag{31}$$

where, θ denotes the angle between an inclined piezoelectric actuator and the x axis (Figure 1). The piezoelectric modulus d_{31}, d_{32}, and d_{36} are dependent on the electrical properties of a piezoelectric material.

Next, substituting equations (19) – (24) into equation (18) and rearrange it for w_{mn} results in equation (32)

$$w_{mn} = \frac{-\sum_{L=1}^{N}\left\{\frac{\alpha_m^2 M^{e}_{xx,L}(\theta)+\beta_n^2 M^{e}_{yy,L}(\theta)}{\alpha_m\beta_n}\right\}A_1(m,L)A_2(n,L) + 2M^{e}_{xy,L}(\theta)B_1(m,L)B_2(n,L)}{D_{11}\left\{\frac{m^4\pi^4}{a^4}\right\} + 2D_3\left\{\frac{m^2n^2\pi^4}{a^2b^2}\right\} + D_{22}\left\{\frac{n^4\pi^4}{b^4}\right\}} \tag{32}$$

where, the terms A_{ij} and B_{ij} for $i,j = \{1,2\}$ are calculated using equations (33) – (36)

$$A_1(m,L) = \cos(\alpha_m x_{1,L}) - \cos(\alpha_m x_{2,L}) \tag{33}$$

$$A_2(n,L) = \cos(\beta_n y_{1,L}) - \cos(\beta_n y_{2,L}) \tag{34}$$

$$B_1(m,L) = \sin(\alpha_m x_{1,L}) - \sin(\alpha_m x_{2,L}) \tag{35}$$

$$B_2(n,L) = \sin(\beta_n y_{1,L}) - \sin(\beta_n y_{2,L}) \tag{36}$$

Finally, substituting equation (32) into equation (16) results in equation (37) which represents the lateral static displacements of the mid-plane ($z = 0$) of a smart laminated simply-supported composite rectangular plate induced by multiple pairs of inclined piezoelectric actuators.

$$w(x,y) = \frac{4}{ab}\sum_{m=1}^{\infty}\sum_{n=1}^{\infty} \left\{\frac{-\sum_{L=1}^{N}\left\{\frac{\alpha_m^2 M^{e}_{xx,L}(\theta)+\beta_n^2 M^{e}_{yy,L}(\theta)}{\alpha_m\beta_n}\right\}A_1(m,L)A_2(n,L) + 2M^{e}_{xy,L}B_1(m,L)B_2(n,L)}{D_{11}\left\{\frac{m^4\pi^4}{a^4}\right\} + 2D_3\left\{\frac{m^2n^2\pi^4}{a^2b^2}\right\} + D_{22}\left\{\frac{n^4\pi^4}{b^4}\right\}}\right\} \times\sin(\alpha_m x)\sin(\beta_n y) \tag{37}$$

The analytical solution developed in this section is implemented in a MATLAB-based computer code to identify twisting deformation response of smart laminated simply-supported composite rectangular plate induced by various inclined piezoelectric actuators. Figure 2 shows the overall process of the analytical solution procedure.

Dynamic deformation response

This part provides a systematic approach toward an investigation into the effect of time-dependent electrical voltage $V(t)$ and piezoelectric excitation frequencies ϕ (Rad/s) on dynamic deformation response of laminated composite rectangular plates excited by various inclined piezoelectric actuators bounded to the host plate with simply-supported boundary condition. The solution procedures in this section are in fact an extension to partial differential equations of static equilibrium in order to take into account the time-dependency of electrical voltage as well as their excitation frequencies.

It is assumed that piezoelectric actuators have an input voltage with sinusoidal oscillation and excitation frequency ϕ. The excitation frequency results in the electrical bending and twisting moments oscillating under the same frequency, leading to the electrical voltage's time-dependency. As such, equation (1) associated with static deformation response of laminated composite plates induced by a set of inclined piezoelectric actuators must be updated to reflect the effect of dynamic deformation response as stated in equation (38)

$$D_{11}\frac{\partial^4 w(x,y,t)}{\partial x^4} + 2D_3\frac{\partial^4 w(x,y,t)}{\partial x^2\partial y^2} + D_{22}\frac{\partial^4 w(x,y,t)}{\partial y^4} + \rho H\frac{\partial^2 w(x,y,t)}{\partial t^2} = \sum_{L=1}^{N} P^{e}_{L}(x,y,\theta)\sin(\phi t) \tag{38}$$

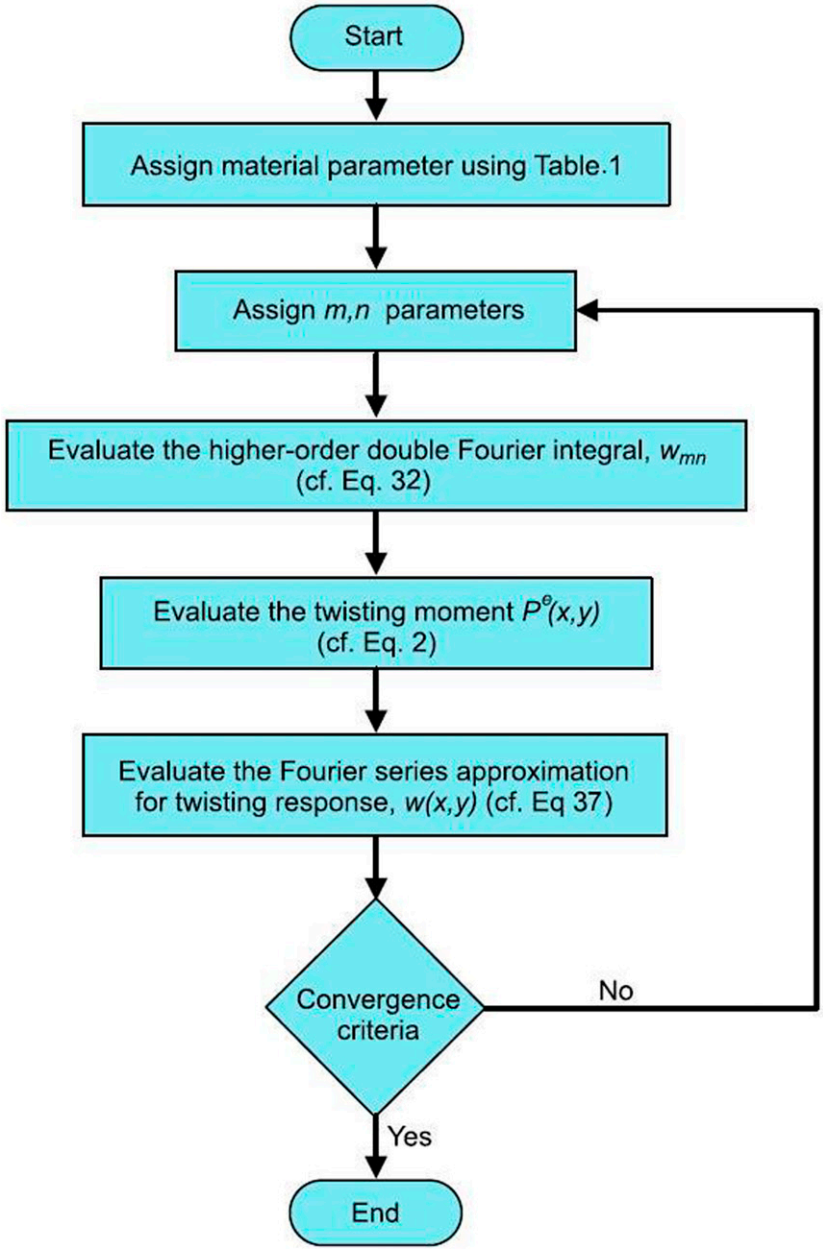

Figure 2. Flowchart for computer implementation of the developed analytical solution procedure to characterize static deformation response of a smart laminated composite rectangular plate induced by multiple inclined piezoelectric actuators.

where,

$$w(x,y,t) = w(x,y) \times \sin(\phi t) = \frac{4}{ab} \sum_{m=1,3,5,\ldots}^{\infty} \sum_{m=1,3,5,\ldots}^{\infty} w_{mn} \sin(\alpha_m x)\sin(\beta_n y)\sin(\phi t) \quad (39)$$

In equation (38), $P_L^e(x,y,\theta)$ was defined earlier in equation (2), ρ and H are density and thickness of a composite plate, respectively, and t(s) is time.

Substituting equation (39) into equation (38) leads to equation (40)

$$D_{11}\frac{\partial^4 w(x,y)}{\partial x^4} + 2D_3\frac{\partial^4 w(x,y)}{\partial x^2 \partial y^2} + D_{22}\frac{\partial^4 w(x,y)}{\partial y^4} - \rho H \phi^2 w(x,y) = \sum_{L=1}^{N} P_L^e(x,y,\theta) \quad (40)$$

Taking double integral Fourier transform over equation (40) and following the procedures discussed earlier, one can finally arrive at equation (41)

$$w(x,y,t) = \frac{4}{ab}\sum_{m=1}^{\infty}\sum_{n=1}^{\infty} \left\{ \frac{\left\{ -\sum_{L=1}^{N} \left\{ \frac{\alpha_m^2 M_{xx,L}^e(\theta) + \beta_n^2 M_{yy,L}^e(\theta)}{\alpha_m \beta_n} \right\} A_1(m,L)A_2(n,L) + M_{xy,L}^e B_1(m,L)B_2(n,L) \right\}}{D_{11}\left\{\frac{m^4\pi^4}{a^4}\right\} + 2D_3\left\{\frac{m^2n^2\pi^4}{a^2b^2}\right\} + D_{22}\left\{\frac{n^4\pi^4}{b^4}\right\} - \rho H \phi^2} \right\} \times \sin(\alpha_m x)\sin(\beta_n y)\sin(\phi t) \tag{41}$$

equation (41) represents dynamic deformation response of a laminated simply-supported composite rectangular plate induced by a set of piezoelectric actuators under an excitation frequency.

Finite element analysis (FEA)

The results obtained from the analytical solution are compared with, and verified by the FEA results determined by Abaqus FEA package.[26] The smart structure is assumed to encompass two parts: (1) The host structure which is modelled as a laminated cross-ply fiber reinforced polymer composite plate and (2) a set of piezoelectric actuators. The piezoelectric actuators are polarized along their thicknesses (along the z axis); therefore, only the piezoelectric coefficients d_{31} and d_{32} are practically in effect.

For a simply-supported plate, the displacements and bending moments are equal to zero along the edges $x = 0$, $x = a$, $y = 0$, and $y = b$. In Abaqus FEA software, U_1, U_2, and U_3 stand for the displacements along the, x, y, and z directions, respectively, and UR_1, UR_2, and UR_3 stand for the rotational angels along the, x, y, and z directions, respectively. Inclination angle between the piezoelectric actuators and host structure is created during the assembly. To intensify the deformation effect of electrical twisting-bending moments and greater actuation result, the piezoelectric actuators are symmetrically bonded with respect to the mid-plane under the same amount of constant electrical voltage but different polarization direction. In general, for an upward displacement, the upper and lower actuators require a negative and positive voltage, respectively, and vice versa (+V and –V applied to the top and bottom, respectively).

In the FEA simulations conducted in this work, Abaqus eight-node, hexahedron, reduced integration, three-dimensional continuum shell elements (SC8R) with hourglass control, and Abaqus eight-node, linear, piezoelectric three-dimensional brick elements (C3D8E) have been assigned to the laminated composite rectangular plates and piezoelectric actuators, respectively. The SC8R elements with three displacement degrees of freedoms (DOFs) per node possess 24 DOFs. The C3D8E elements with three displacement DOFs and one electric voltage DOF per node have a total of 32 DOFs to be specified during the numerical solution process.[27] It is important to note that the piezoelectric actuators are directly attached to the laminated composite rectangular plates using the tie constraint available in Abaqus/Standard (i.e. without any interfacial layer),[26] which allows the existence of a mesh nonconformity between the piezoelectric actuators and laminated composite rectangular plate (host structure). It is also important to emphasize that a mesh refinement study has been performed to find the appropriate mesh densities to minimize the numerical analysis's approximation error.

Analytical solution validation and convergence study (θ = 0°)

This section aims to validate the developed analytical solution as well as convergence study of the present work by comparing the proposed analytical solution with the results of the published literature for the particular cases, when the angle of twist is zero (θ = 0°). Since the literature lacks the case studies in which inclination angle is considered ($\theta \neq 0°$), the electro-mechanical twisting deformation under both static and time-dependent electrical loads is validated by Abaqus FEA package later on in the next section.

Consider a smart laminated cross-ply carbon/epoxy composite plate induced by a pair of PZT G-1195 actuators with inclination angle $\theta = 0°$. The plate dimensions are set as a = 3.38 (m), b = 0.3 (m), and H = 1.5876 (m). The laminate encompasses four layers with stacking sequence of [0/90/90/0]. The composite layers have equal thickness. This is apparently a special case in which the piezoelectric actuators induce pure electrical bending due to a zero inclination angle, resulting in pure flexural deformation of the laminated composite plate. The material properties of the composite laminate and piezoelectric material are provided in Table 1.

Table 1. Summary of the electro-mechanical parameters associated with carbon/epoxy composite and PZT G-1195 piezoelectric materials.

Material properties	PZT G-1195[27,28]	Carbon/epoxy composite[27]
E_1 (GPa)	63	108
E_2 (GPa)	63	10.3
ν_{12}	0.3	0.28
G_{12} (GPa)	24.23	7.13
G_{13} (GPa)	24.23	7.13
G_{23} (GPa)	24.23	4.02
ρ (Kg/m^3)	7600	1600
d_{31} (V/m)	1.9×10^{-10}	—
d_{32} (V/m)	1.9×10^{-10}	—
ρ_z (F/m)	15×10^{-9}	—

Table 2. w_{max} in the composite plate induced by a pair of piezoelectric actuators of various sizes when piezoelectric thickness is kept constant as $t_{pe} = 0.1H$ and inclination angle is $\theta = 0°$ (pure bending deformation).

	$w_{max} \times 10^{-6}$ (m)						
	Present study						
Piezoelectric size (m^2)	$n = m = 5$	$n = m = 10$	$n = m = 20$	$n = m = 30$	Ansys[27]	FEM[27]	Rits[27]
0.06 × 0.04	0.982	1.124	1.130	1.182	1.170	1.197	1.208
0.08 × 0.06	1.968	1.987	2.016	2.104	2.050	2.076	2.087
0.10 × 0.08	2.897	2.984	3.067	3.108	3.030	3.049	3.054

Table 3. w_{max} in the composite plate induced by a pair of piezoelectric actuators of various thicknesses when the piezoelectric size is kept constant as 0.08 × 0.06 (m^2) and inclination angle is $\theta = 0°$ (pure bending deformation).

	$w_{max} \times 10^{-6}$ (m)						
	Present study						
t_{pe}/H	$n = m = 5$	$n = m = 10$	$n = m = 20$	$n = m = 30$	Bending moment model[27]	Refined model[27]	FEM[27]
0.1	1.704	1.789	1.822	1.896	1.894	2.087	2.076
0.4	0.657	0.689	0.722	0.759	0.709	0.8131	0.788
0.8	0.283	0.294	0.311	0.347	0.308	0.378	0.367
1	0.189	0.195	0.203	0.264	0.224	0.280	0.273

Table 4. w_{max} in the composite plate induced by a pair of piezoelectric actuators of various sizes when the piezoelectric actuators are subjected to various excitation frequencies. Inclination angle is $\theta = 0°$ (pure bending deformation).

		w_{max} (mm)				
		Present study				
Piezoelectric size (m^2)	Excitation frequency ϕ (rad/s)	n = m = 10	$n = m = 20$	$n = m = 30$	FEM[29]	Analytical[29]
0.06 × 0.04	350	3.25×10^{-2}	3.28×10^{-2}	3.32×10^{-2}	3.53×10^{-2}	3.33×10^{-2}
0.08 × 0.06		1.49×10^{-1}	1.52×10^{-1}	1.54×10^{-1}	1.66×10^{-1}	1.56×10^{-1}
0.10 × 0.08		0.87	0.97	1.04	1.15	1.06
0.06 × 0.04	650	0.41×10^{-3}	0.43×10^{-3}	0.48×10^{-3}	0.51×10^{-3}	0.50×10^{-3}
0.08 × 0.06		0.84×10^{-2}	0.91×10^{-2}	0.96×10^{-2}	0.10×10^{-2}	0.98×10^{-2}
0.10 × 0.08		0.93×10^{-2}	0.11×10^{-2}	0.13×10^{-2}	0.15×10^{-2}	0.15×10^{-2}
0.06 × 0.04	870	5.88×10^{-4}	6.12×10^{-4}	6.36×10^{-4}	5.95×10^{-4}	6.42×10^{-4}
0.08 × 0.06		7.95×10^{-4}	8.21×10^{-4}	8.43×10^{-4}	7.74×10^{-4}	8.49×10^{-4}
0.10 × 0.08		0.87×10^{-3}	0.98×10^{-3}	1.10×10^{-3}	1.17×10^{-3}	1.12×10^{-3}

Table 5. Quantitative comparison (i.e. *R*-squared correlation coefficient) of the proposed analytical solution procedure versus the FEA results.

	x axis			*y* axis		
—	$\theta = 0°$	$\theta = 45°$	$\theta = 90°$	$\theta = 0°$	$\theta = 45°$	$\theta = 90°$
One pair of actuators	0.998	0.990	0.988	0.997	0.989	0.991
Two pairs of actuators	0.994	0.993	0.994	0.996	0.995	0.994

Table 6. Summary of the electro-mechanical parameters associated with the composite and piezoelectric materials used in the current study.

Material properties	KYNAR[30]	T300/976 GFRP[31]
E_1 (GPa)	2	150
E_2 (GPa)	2	9
ν_{12}	0.29	0.3
G_{12} (GPa)	0.77	7.1
G_{13} (GPa)	0.77	7.1
G_{23} (GPa)	0.77	2.5
ρ (Kg/m^3)	1780	1600
d_{31} (V/m)	2.3×10^{-11}	—
d_{32} (V/m)	4.6×10^{-12}	—
ρ_z (F/m)	0.1062×10^{-9}	—

Table 2 and Table 3 show the results comparison with the published literature when piezoelectric actuators of various sizes and thicknesses are considered. It is noticed that a good agreement between the present work and the literature is observed and convergence can be achieved with a small number of Fourier terms.

Now consider a smart laminated cross-ply carbon/epoxy composite plate dynamically induced by a pair of PZT G-1195 actuators with inclination angle $\theta = 0°$. This time, a time-dependent electrical voltage with the electrical voltage of $V = 1$ (V) and $V = -1$ (V) is applied to the top and bottom piezoelectric actuators, respectively. Like the static case-study, the plate dimensions are set as $a = 3.38$ (m) and $b = 0.3$ (m) and $H = 1.5876$ (m). The laminate encompasses four layers with stacking sequence of [0/90/90/0], like the static case-study.

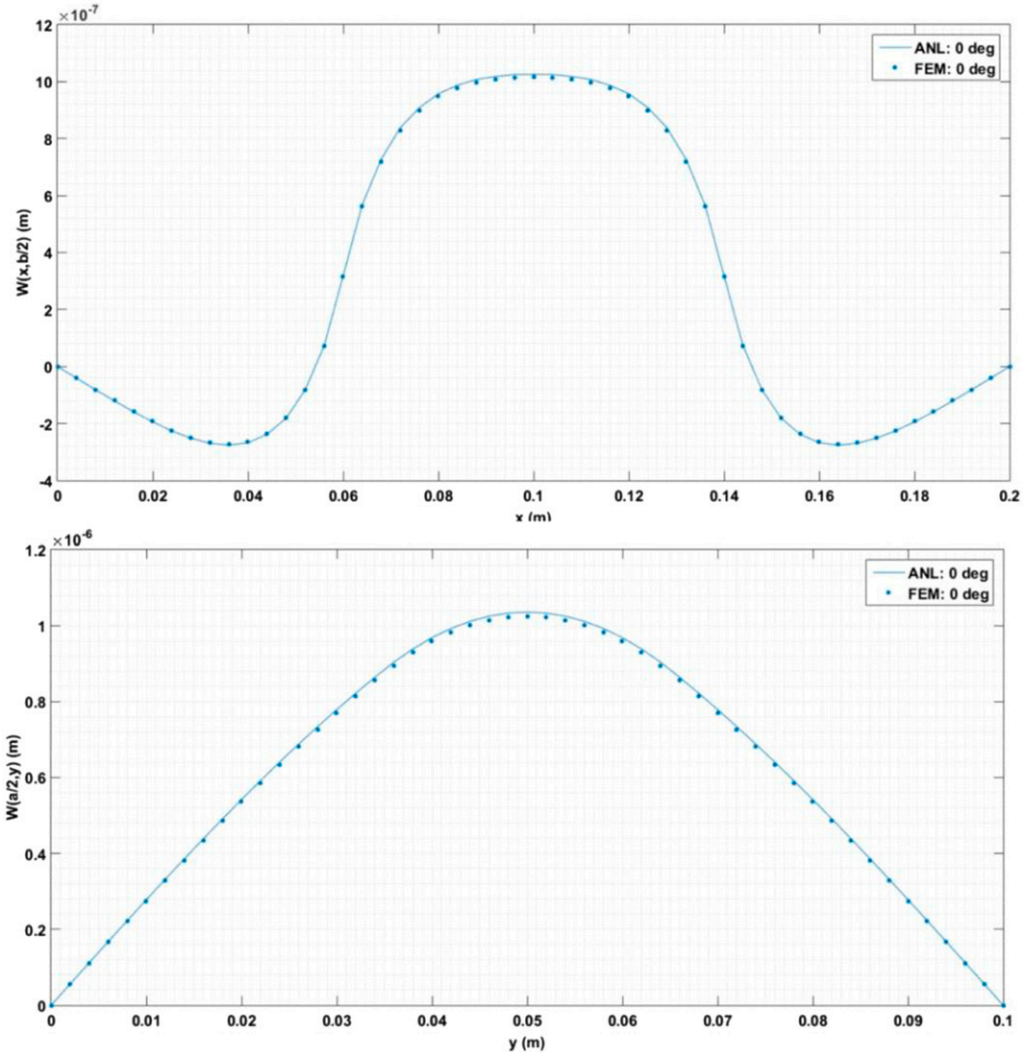

Figure 3. Smart laminated composite plate induced by a pair of inclined piezoelectric actuators ($\theta = 0°$).

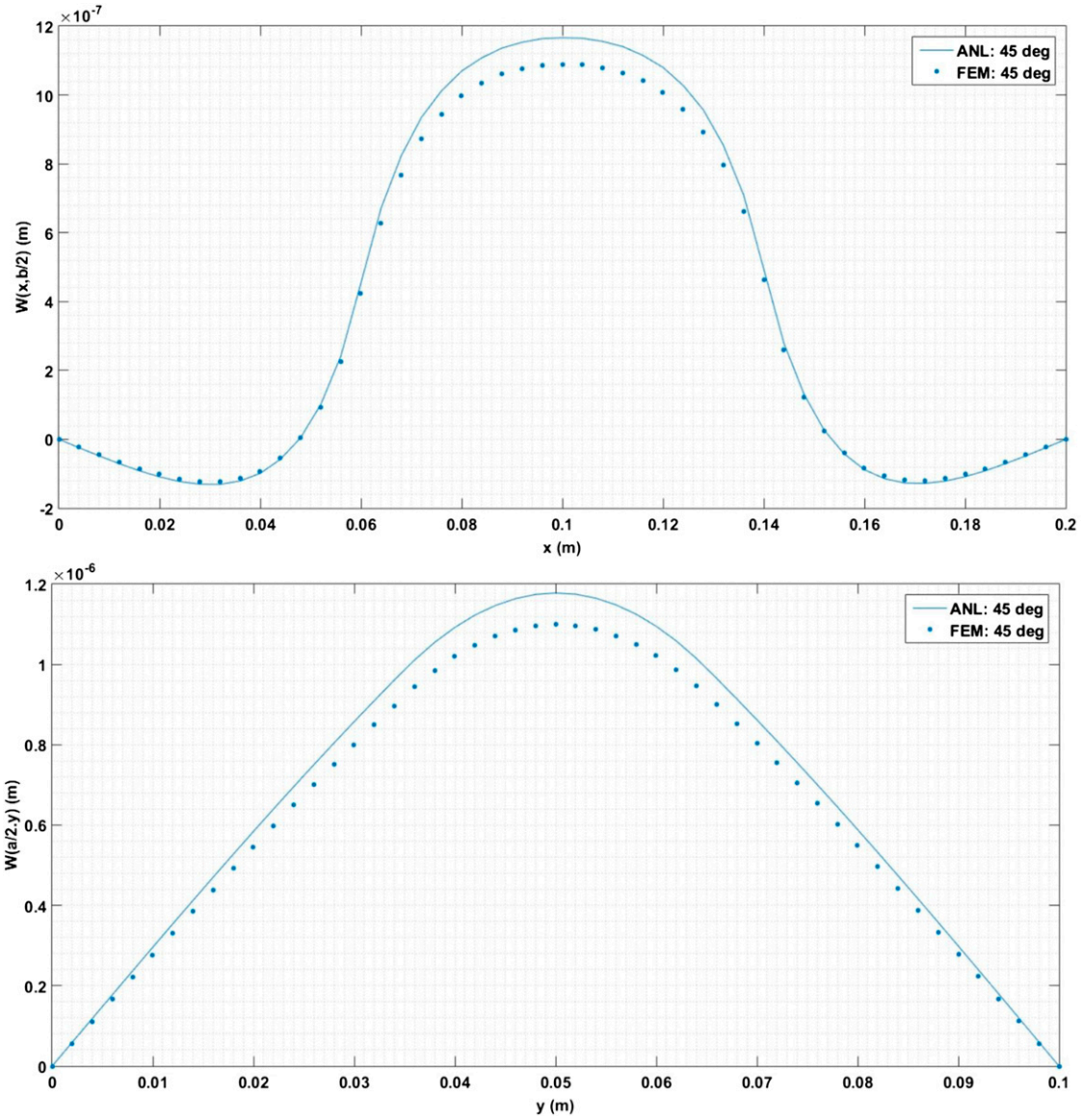

Figure 4. Smart laminated composite plate induced by a pair of inclined piezoelectric actuators (θ = 45°).

Table 4 shows the results comparison with the published literature when piezoelectric actuators are subjected to various excitation frequencies of $\phi = \{350,650,870\}$ (rad/s), respectively. The convergence study shows a good agreement with the published data in the literature.

Static deformation response for inclination angle $\theta \neq 0°$

This section provides an evaluation of the predictive capability of the analytical solution procedure developed and its computer implementation to determine static deformation response of smart laminated simply-support composite rectangular plates induced by single pair or multiple pairs of inclined piezoelectric actuators. The analytical results are compared with, and verified by Abaqus FEA package. The reason behind this is because there is no case-study in the published literature that has investigated the effect of inclination angle ($\theta \neq 0°$) on static and dynamic deformation response of laminated simply-supported composite plates induced by inclined piezoelectric actuators.

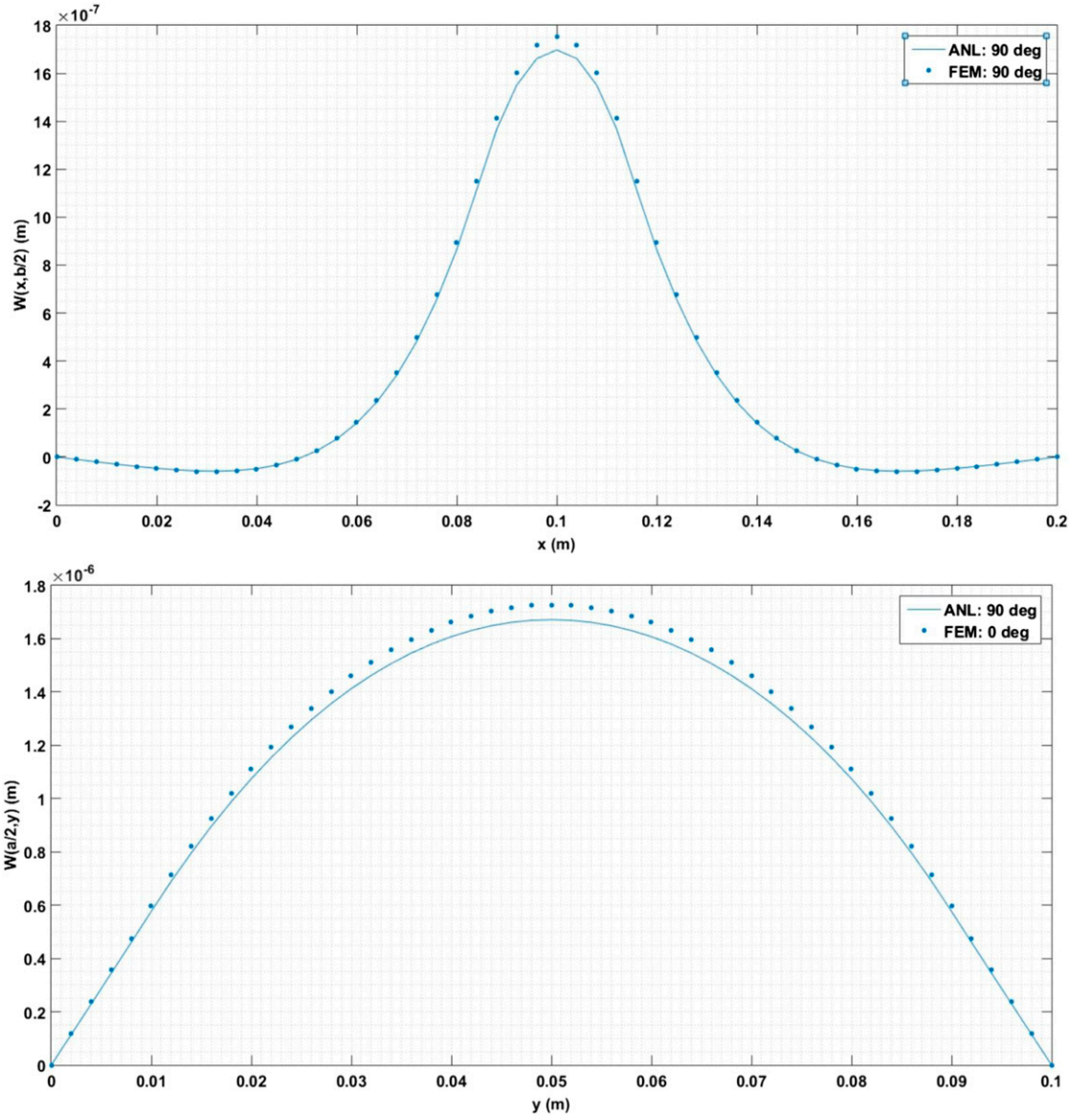

Figure 5. Smart laminated composite plate induced by a pair of inclined piezoelectric actuators (θ = 90°).

It should be noted that the detailed quantitative comparison (i.e. R-squared correlation coefficient) between the analytical and FEA results has been summarized in Table 5.

In this section, KYNAR piezoelectric film is considered to create twisting deformation in laminated composite plates due to its unique electrical properties ($d_{31} \neq d_{32}$). The elastic and electrical properties of KYNAR piezoelectric film can be found in Table 6

One pair of inclined piezoelectric actuators

In this layout, a single pair of inclined piezoelectric actuators is attached to the top and bottom surfaces of a smart laminated composite rectangular plate. As mentioned earlier, simply-supported constraints are prescribed at all four edges of the composite plate. The composite plate's static deformation response is investigated for three different inclination angles (i.e. $\theta = 0^o$, $\theta = 45^o$ and $\theta = 90^o$). The top and bottom piezoelectric actuators are subjected to +300 (V) and −300 (V) electrical voltage, respectively.

The plate dimensions are $a = 0.2$ (m) and $b = 0.1$ (m) and the plate's stacking sequence configuration is assumed to be [90/0/90]. Each composite layer has 0.3 (mm) thickness, therefore the plate's total thickness is $H = 1.2$ (mm). The piezoelectric actuators are 0.08 (m) in length and 0.03 (m) in width and have 0.2 (mm) thickness.

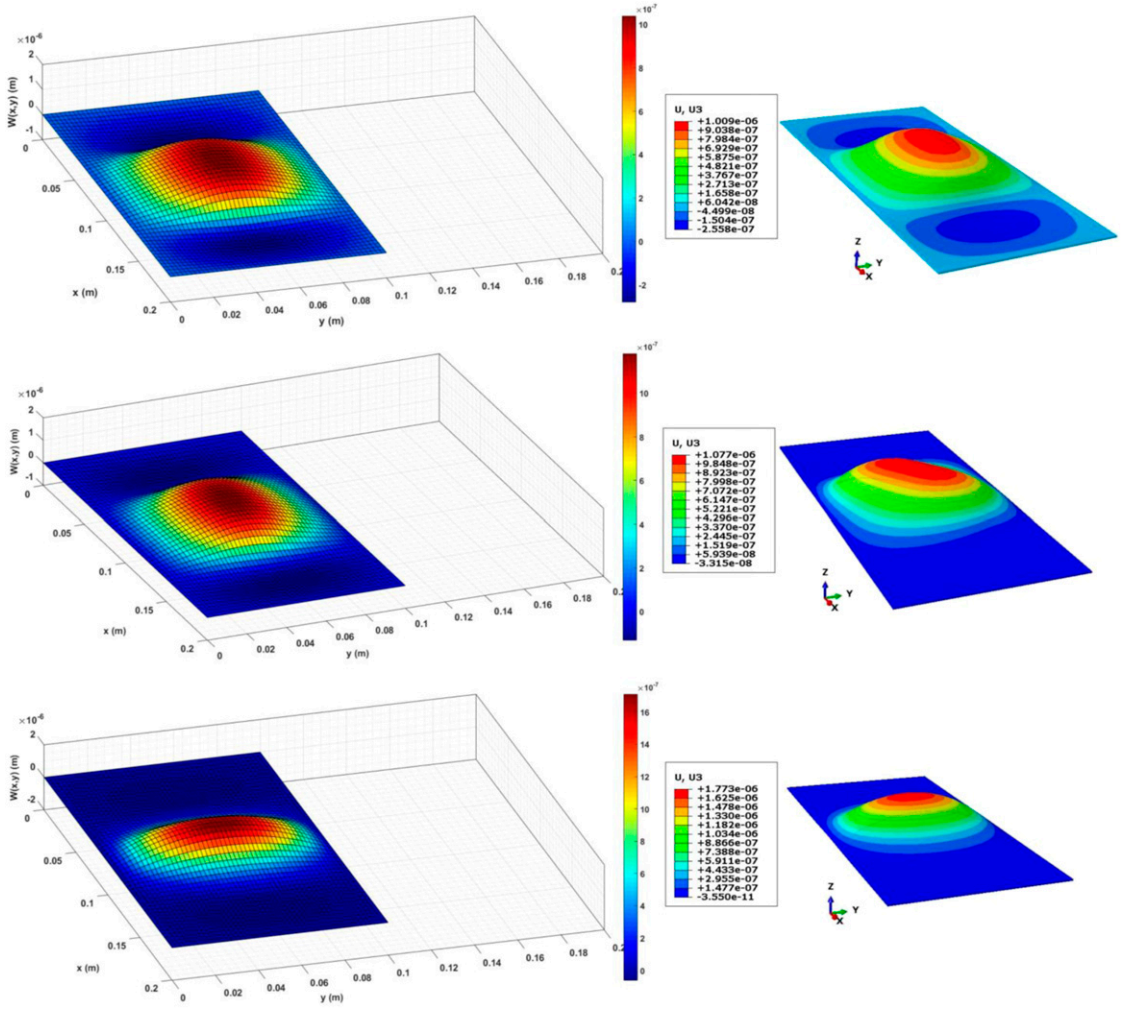

Figure 6. The 3D contour plots of twisting response for a smart laminated composite rectangular plate induced by one pair of inclined piezoelectric actuators obtained from the analytical solution developed in *The Analytical solution procedures* (left) and the optimally-converged FEA (right): From top to bottom, the piezoelectric inclination angles are $\theta = 0^{\circ}$, $\theta = 45^{\circ}$, and $\theta = 90^{\circ}$, respectively.

Figure 3 shows the static displacement curves of a smart laminated composite rectangular plate induced by a single pair of piezoelectric actuators with an inclination angle of $\theta = 0^{\circ}$ along $y = a/2$ and $x = a/2$ paths. Figure 4 and Figure 5 are similar to Figure 3 except that the static displacement curves correspond to inclination angles of $\theta = 45^{\circ}$ and $\theta = 90^{\circ}$, respectively. To further demonstrate the predictive capabilities of the proposed analytical solution procedure, Figure 6 provides a comparison between the analytical and numerical results associated with the three-dimensional (3D) static deformation response of smart laminated composite rectangular plates induced by a single pair of the piezoelectric actuators with inclination angles of $\theta = 0^{\circ}$, $\theta = 45^{\circ}$, and $\theta = 90^{\circ}$, respectively. The results associated with the proposed analytical procedures show good agreement on account of having a good correlation with the data obtained from the optimally-converged FEA simulations. It can be observed that the effect of inclination angle on static deformation response is insignificant when one pair of inclined piezoelectric actuators is selected.

Two pairs of inclined piezoelectric actuators

The capability of the analytical solution procedure developed is further probed by comparing the analytically-determined

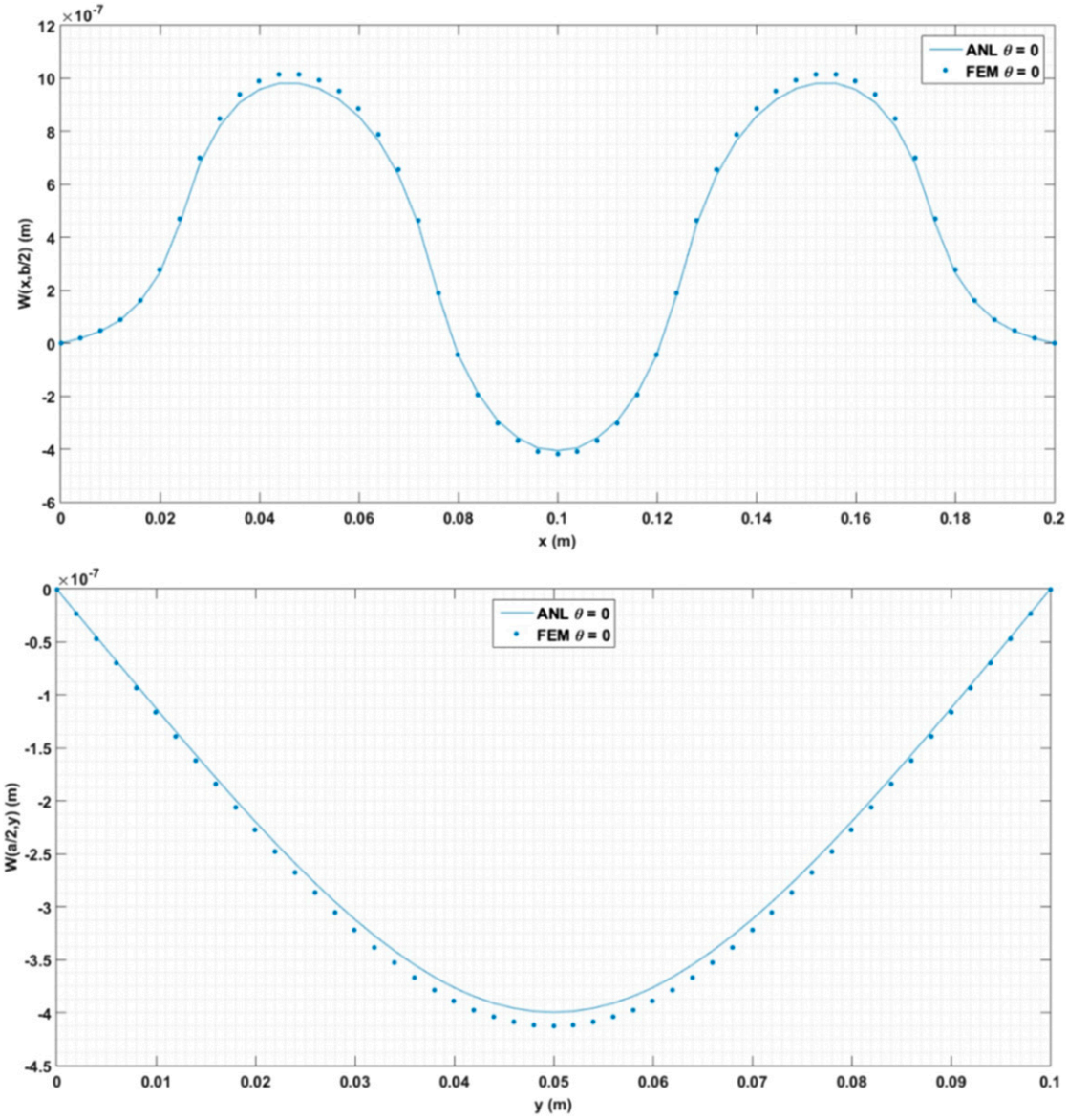

Figure 7. Smart laminated composite plate induced by two pairs of inclined piezoelectric actuators (θ = 0°).

static twisting response of a smart laminated composite rectangular plate induced by two pairs of inclined piezoelectric actuators with the numerical data obtained from FEA. The top and bottom piezoelectric actuators are subjected to +300 (V) and −300 (V) electrical voltage, respectively.

The plate dimensions are a = 0.2 (m) and b = 0.1 (m). Each composite layer has 0.3 (mm) thickness, therefore the plate's total thickness is H = 0.9 (mm). The piezoelectric actuators are 0.05 (m) in length and 0.025 (m) in width and have 0.2 (mm) thickness. Stacking sequence configuration of the laminated composite plate is [90,0,90].

Figures 7–9 show the static displacement curves of a smart laminated composite rectangular plate induced by two pair of inclined piezoelectric actuators with an inclination angle of $\theta = 0^o$, $\theta = 45^o$, and $\theta = 90^o$, respectively along $y = a/2$ and $x = a/2$ paths. Figure 10 shows a comparison between the analytical and numerical results associated with the three-dimensional (3D) static deformation response of smart laminated composite rectangular plates induced by two pairs of inclined piezoelectric actuators with inclination angles of $\theta = 0^o$, $\theta = 45^o$, and $\theta = 90^o$, respectively. It can be ascertained that the presently-developed analytical solution can accurately predict twisting response on accord of having an infinitesimal variation with the curves reproduced by FEA. It should also be essential to note that the analytically-determined curves and the ones obtained from the FEA

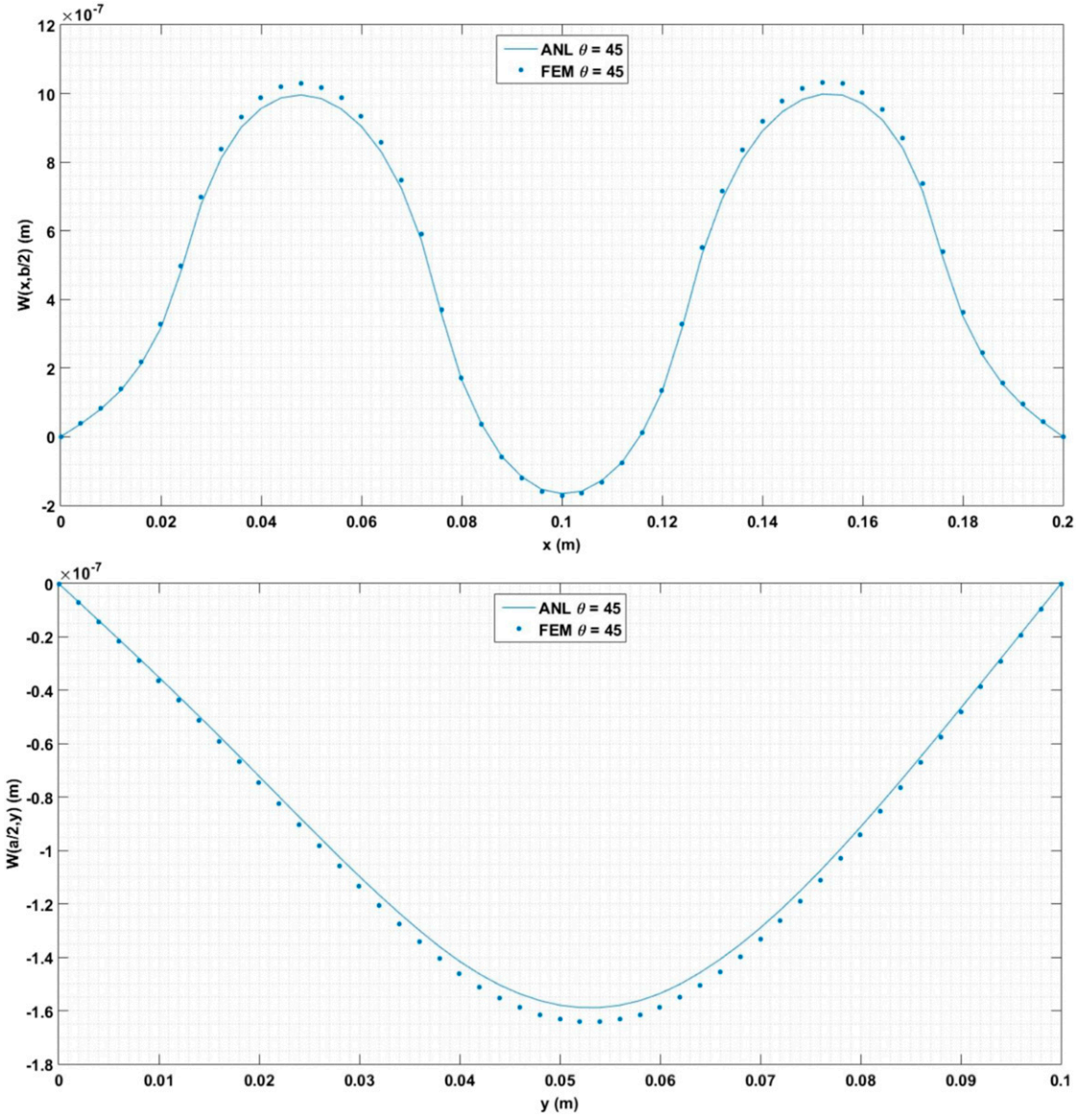

Figure 8. Smart laminated composite plate induced by two pairs of inclined piezoelectric actuators (θ = 45°).

simulations are indistinguishable by approaching the plate's boundaries. Like the results earlier, it can be observed that the effect of inclination angle of static deformation response is insignificant when two pairs of inclined piezoelectric actuators are selected.

Dynamic deformation response for inclination angle $\theta \neq 0°$

This section provides an evaluation of the predictive capability of the analytical solution procedure developed and its computer implementation to characterize dynamic deformation response of smart laminated simply-support composite rectangular plates induced by inclined piezoelectric actuators.

Two case studies are to be explored: the host structure integrated with (1) a pair of inclined piezoelectric actuators and (2) double pairs of inclined piezoelectric actuators. The vibration displacements associated with each case study is explored based on the proposed analytical and FEA studies. Same detailed quantitative comparison (i.e. R-squared correlation coefficient), provided in Table 2, is used for dynamic analysis.

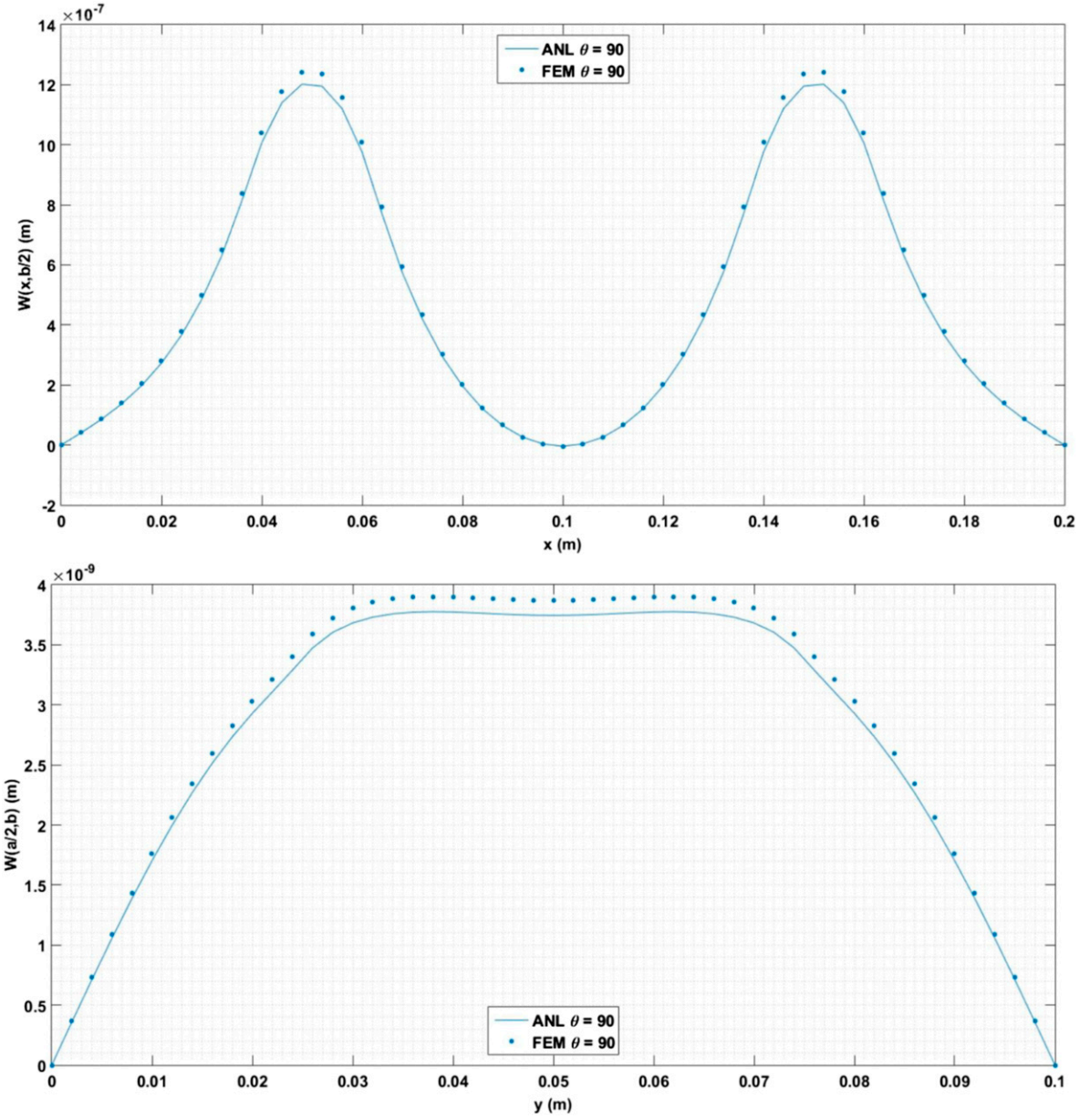

Figure 9. Smart laminated composite plate induced by two pairs of inclined piezoelectric actuators (θ = 90°).

One pair of inclined piezoelectric actuators

In this layout, a single pair of inclined piezoelectric actuators is attached to the top and bottom surfaces of a smart laminated composite rectangular plate and dynamic deformation response is investigated for four different inclination angles (i.e. $\theta = 0^o$, $\theta = 45^o$, $\theta = 75^o$, and $\theta = 90^o$).

In the following case study examples, dynamic deformation response of smart laminated composite plate induced by one pair of inclined piezoelectric actuators under three different excitation frequencies ϕ = {350,800,1200} (rad/s) is explored. The excitation frequencies are selected in such a way that transits from low to high frequency.

The plate dimensions are selected as $a = 0.2$ (m) and $b = 0.1$ (m). Each composite layer has 0.3 (mm) thickness, therefore the plate's total thickness is $H = 0.9$ (mm). The piezoelectric actuators are 0.08 (m) in length and 0.03 (m) in width and have 0.2 (mm) thickness. It is assumed that the composite plate is made of symmetrical laminate with stacking sequence configuration of [90,0,90].

Figures 11–13 show the vibration displacements curves at the center ($x = a/2$ (m) and $y = b/2$ (m)) of a smart

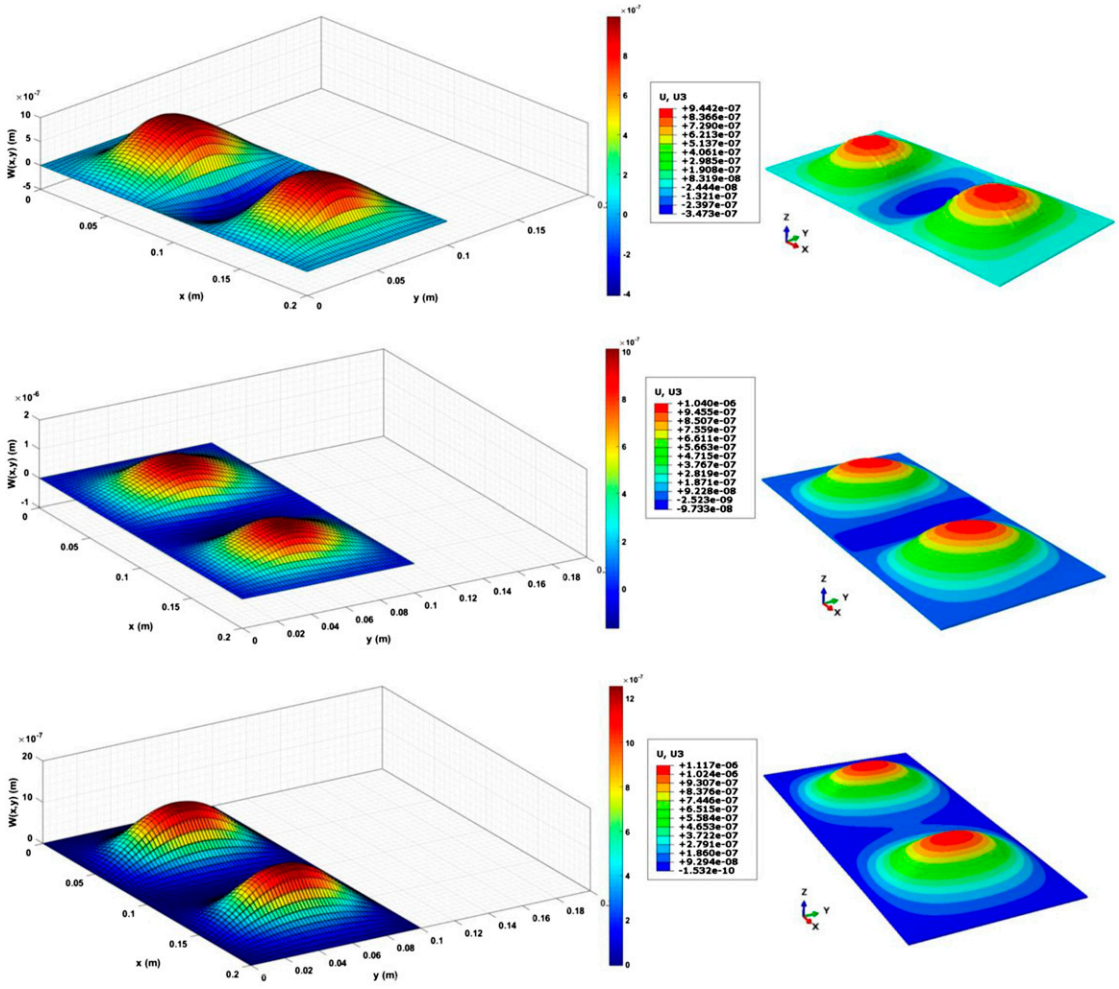

Figure 10. The 3D contour plots of twisting response for a smart laminated composite rectangular plate induced by two pairs of inclined piezoelectric actuators obtained from the analytical solution developed in *The Analytical solution procedures* (left) and the optimally-converged FEA (right): From top to bottom, the piezoelectric inclination angles are $\theta = 0°$, $\theta = 45°$, and $\theta = 90°$, respectively.

laminated composite rectangular plate induced by a single pair of inclined piezoelectric actuators excited under the excitation frequencies of $\phi = 350$ (rad/s), $\phi = 800$ (rad/s), and $\phi = 1200$ (rad/s), respectively.

The results comparison between the developed analytical procedures and FEA show good agreement. Figure 14 shows the laminated composite plate's mode shape at $t = T/4$ (s), where T is the period of vibration, based on the analytical procedures and the optimally-converged FEA simulations. Figure 14 is a particular case when inclination angle of piezoelectric actuators is $\theta = 45^{o}$. The effect of piezoelectric actuators' excitation frequency on maximum amplitude of vibration can be observed in Figure 14. Unlike static deformation response, the effect of inclination angle on dynamic deformation response is significant.

Two pairs of inclined piezoelectric actuators and various input voltages

This section investigates the effect of multiple pairs of inclined piezoelectric actuators with distinct input voltages on dynamic deformation response of laminated composite plates. To do so, two pairs of piezoelectric actuators are attached to the top and bottom surfaces of a smart laminated composite

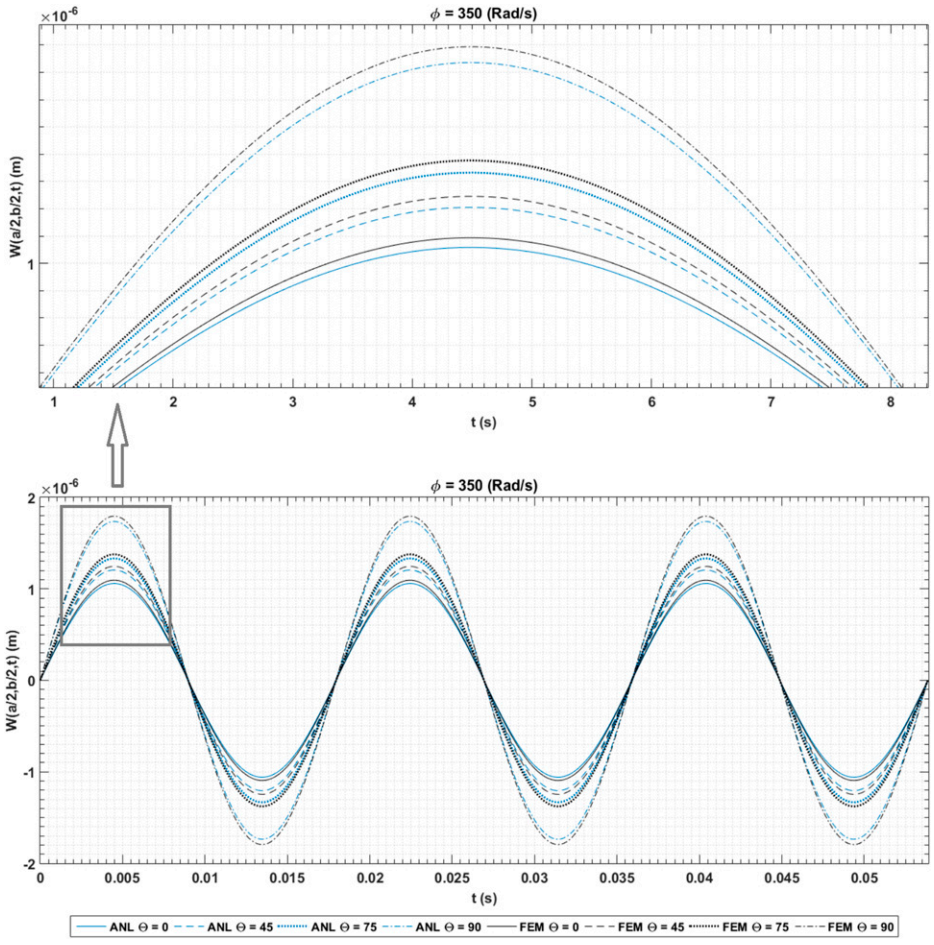

Figure 11. Vibration displacements curves at the center ($x = a/2$ (m) and $y = b/2$ (m)) of a smart laminated composite rectangular plate induced by a single pair of inclined piezoelectric actuators excited under the excitation frequency of $\phi = 350$ (rad/s) based on the developed analytical solution and Abaqus FEA.

rectangular plate. To observe the sole effect of actuator number and distinct input voltages on dynamic deformation response, inclination angle and excitation frequency are kept constant at $\theta = 45^{o}$ and $\phi = 350$ (rad/s), respectively.

The plate dimensions are $a = 0.2$ (m) and $b = 0.1$ (m). Each composite layer has 0.3 (mm) thickness, therefore the plate's total thickness is $H = 0.9$ (mm). The piezoelectric actuators are 0.05 (m) in length and 0.025 (m) in width and have 0.2 (mm) thickness. Stacking sequence of the laminated composite plate is [90,0,90].

In the first attempt, 300 (V) and −300 (V) are applied to the top and bottom piezoelectric actuators, respectively. In the second attempt, the first and the second piezoelectric actuators at the top are subjected to the voltages of 300 (V) and 150 (V), respectively. Same voltages are applied to the first and second piezoelectric actuators at the bottom, but with the negative value.

The force vibration displacements result at the center ($x = a/2$ (m) and $y = b/2$ (m)) of the plate associated with both cases has been plotted against time in Figure 15 based on the proposed analytical procedures and optimally converged FEA. The results from both approaches demonstrate that the effect of variation of the input voltage on dynamic deformation response is significant. The laminated composite plate's mode shape with maximum amplitude associated with the cases discussed above is shown in Figure 16 based on the proposed analytical procedures and optimally-converged FEA.

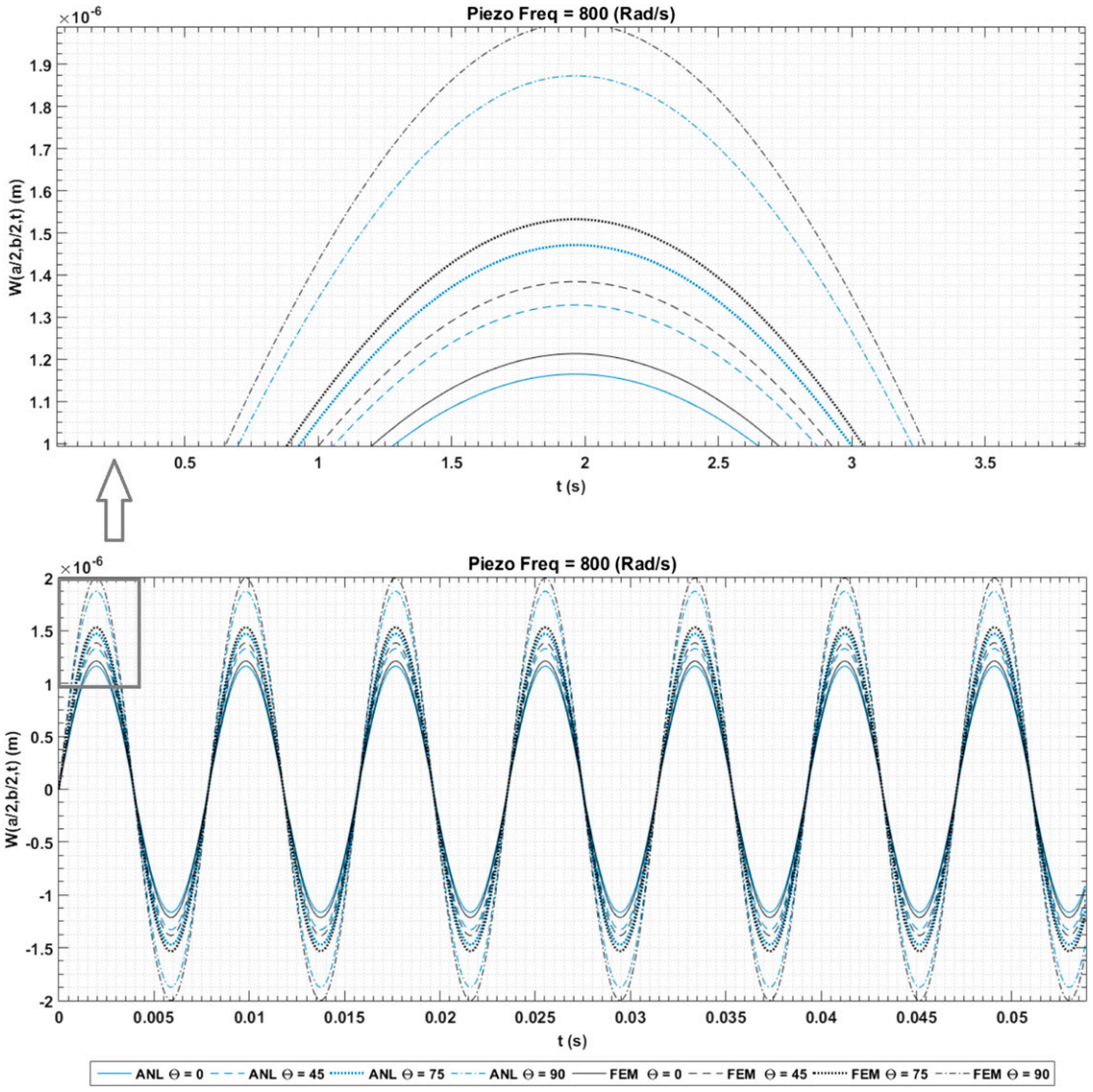

Figure 12. Vibration displacements curves at the center ($x = a/2$ (m) and $y = b/2$ (m)) of a smart laminated composite rectangular plate induced by a single pair of inclined piezoelectric actuators excited under the excitation frequency of ϕ = 800 (rad/s) based on the developed analytical solution and Abaqus FEA.

Effect of excitation frequency on maximum amplitude of vibration

In this layout, the effect of excitation frequency of inclined piezoelectric actuators on maximum amplitude of vibration is investigated. A single pair of piezoelectric actuators is bounded to the top and bottom surfaces of a laminated composite plate. The plate dimensions are a = 0.2 (m) and b = 0.1 (m). The composite plate has three layers with stacking sequence configuration of [90,0,90]. Each composite layer has 0.3 (mm) thickness, therefore the plate's total thickness is H = 0.9 (mm). The piezoelectric actuators are 0.08 (m) in length and 0.03 (m) in width and have 0.2 (mm) thickness.

The piezoelectric actuators, placed at the centroid of the top and bottom faces of the laminated composite plate, are subjected to various excitation frequencies within a finite range of ϕ = [0–1000] (rad/s) and maximum amplitude of vibration corresponding to each excitation frequency is then plotted as shown in Figure 17.

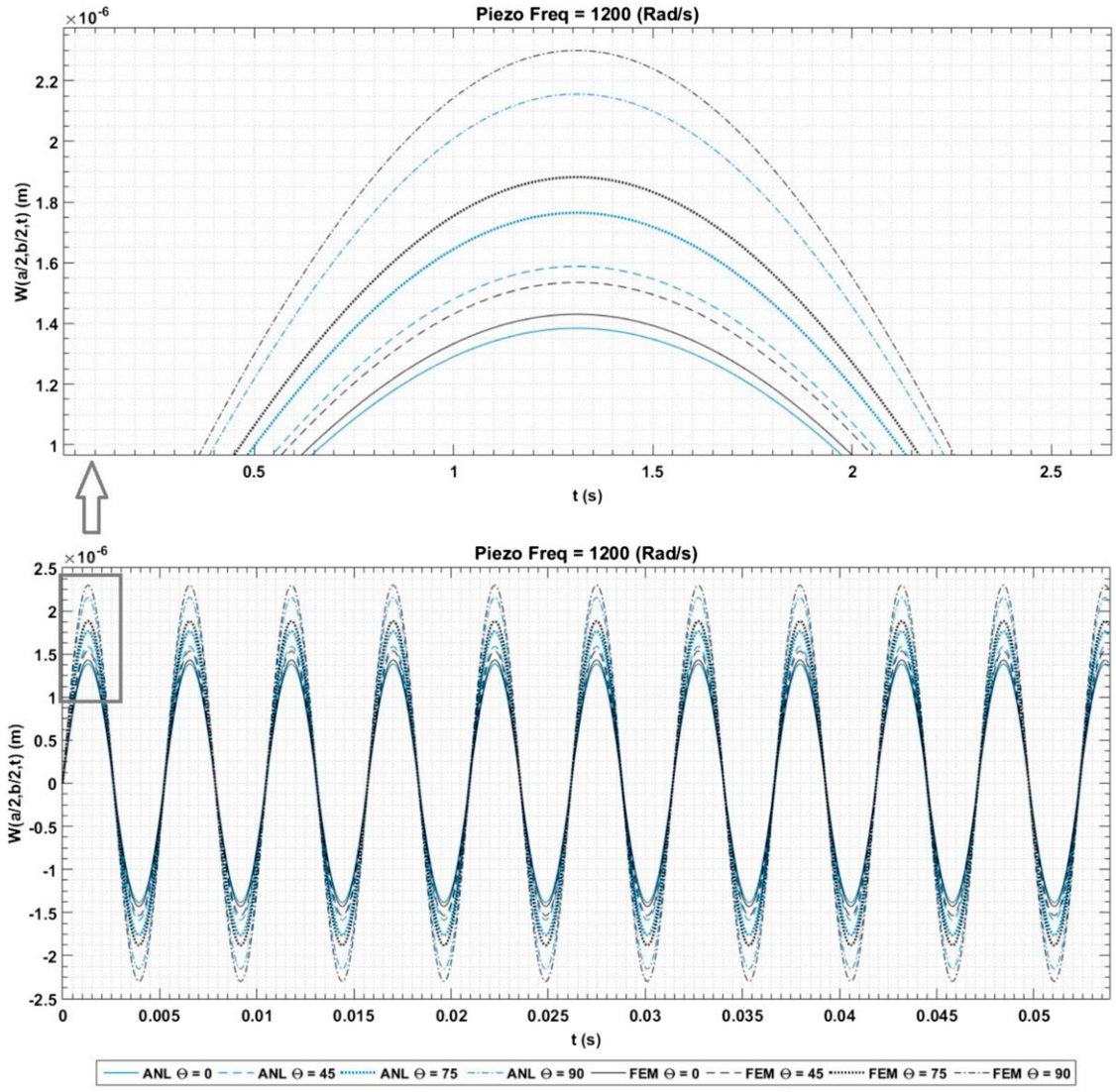

Figure 13. Vibration displacements curves at the center ($x = a/2$ (m) and $y = b/2$ (m)) of a smart laminated composite rectangular plate induced by a single pair of inclined piezoelectric actuators excited under the excitation frequency of $\phi = 1200$ (rad/s) based on the developed analytical solution and Abaqus FEA.

The analytical results demonstrate that an increase in the excitation frequency results in maximum amplitude of vibration increasing in a nonlinear fashion. Although, the nonlinear increase associated with maximum amplitude of vibration demonstrates to be irrespective of inclination angle of piezoelectric actuators, maximum amplitude of vibration is significantly higher for any particular excitation frequency when inclination angle is $\theta = 90°$.

Concluding remarks

A Levi-type analytical solution procedure was developed to analyze twisting deformation response of smart laminated composite plates under static and dynamic conditions. Twisting deformation was caused by inclination angle between the piezoelectric actuators and the x axis. The key to development of this analytical solution procedure was to

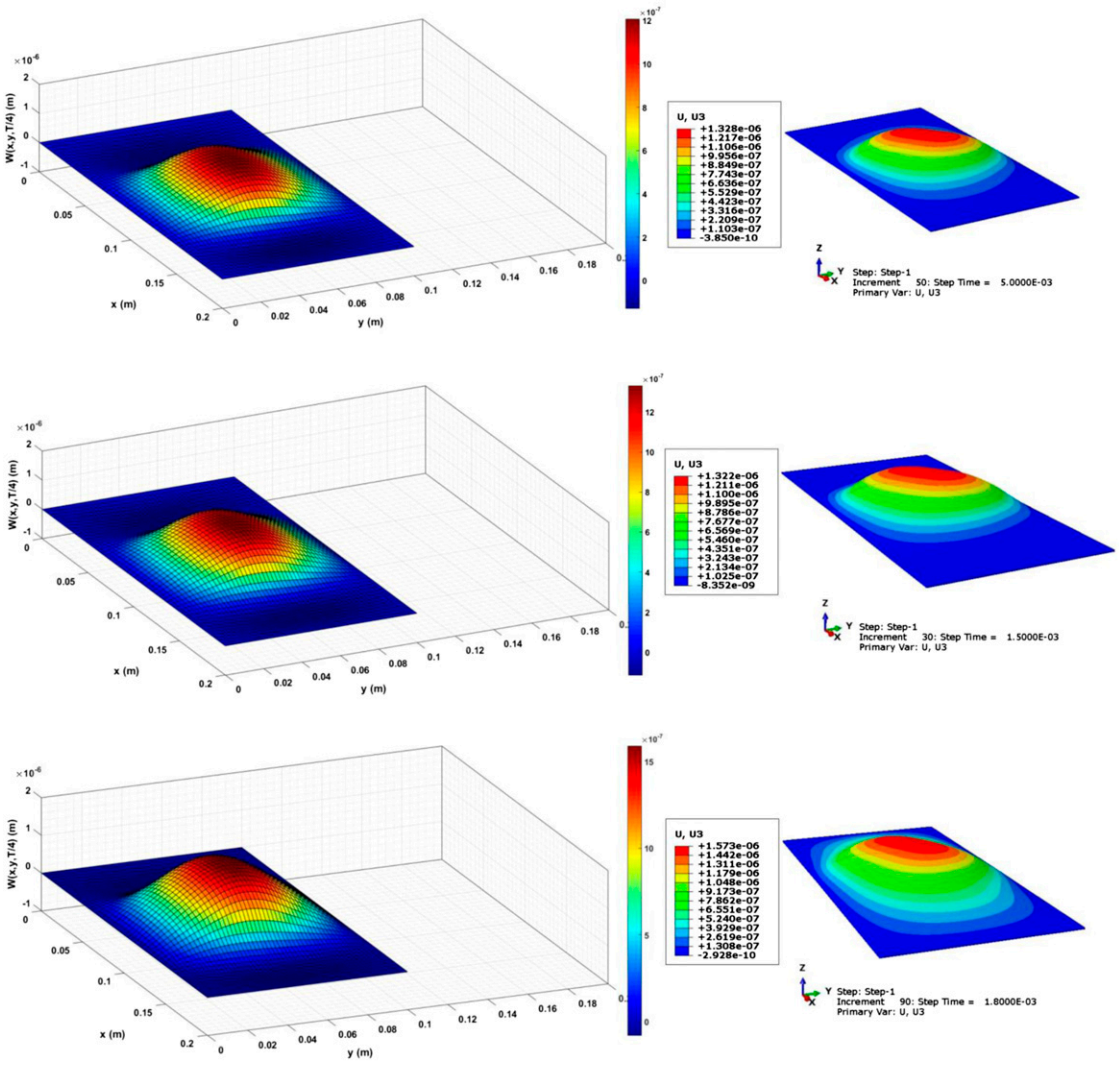

Figure 14. 3D contour plots of dynamic deformation response of a smart laminated composite rectangular plate induced by a pair of inclined piezoelectric actuators under various excitation frequencies based on the analytical solution (left) and the optimally-converged FEA (right): From top to bottom, the excitation frequencies are ϕ = 350 (rad/s), ϕ = 800 (rad/s), and ϕ = 1200 (rad/s), respectively.

employ double finite integral multivariable Fourier transform method coupled with discretized higher order partial differential unit step function equations. The proposed analytical solution procedure was implemented computationally through a Matlab-based computer code.

The accuracy of the developed analytical solution procedures was initially tested through convergence study and results comparison with the published literature for a particular case when inclination angle is θ = 0°. This demonstrated to be a special case study in which twisting deformation does not exist and static and dynamic deformation responses are due to pure bending moment induced by piezoelectric actuators. The results comparison showed good agreement. The convergence study demonstrated that convergence could easily be achieved by selecting small values for Fourier terms m and n.

There is no published benchmark data in this context for the developed analytical results validation when

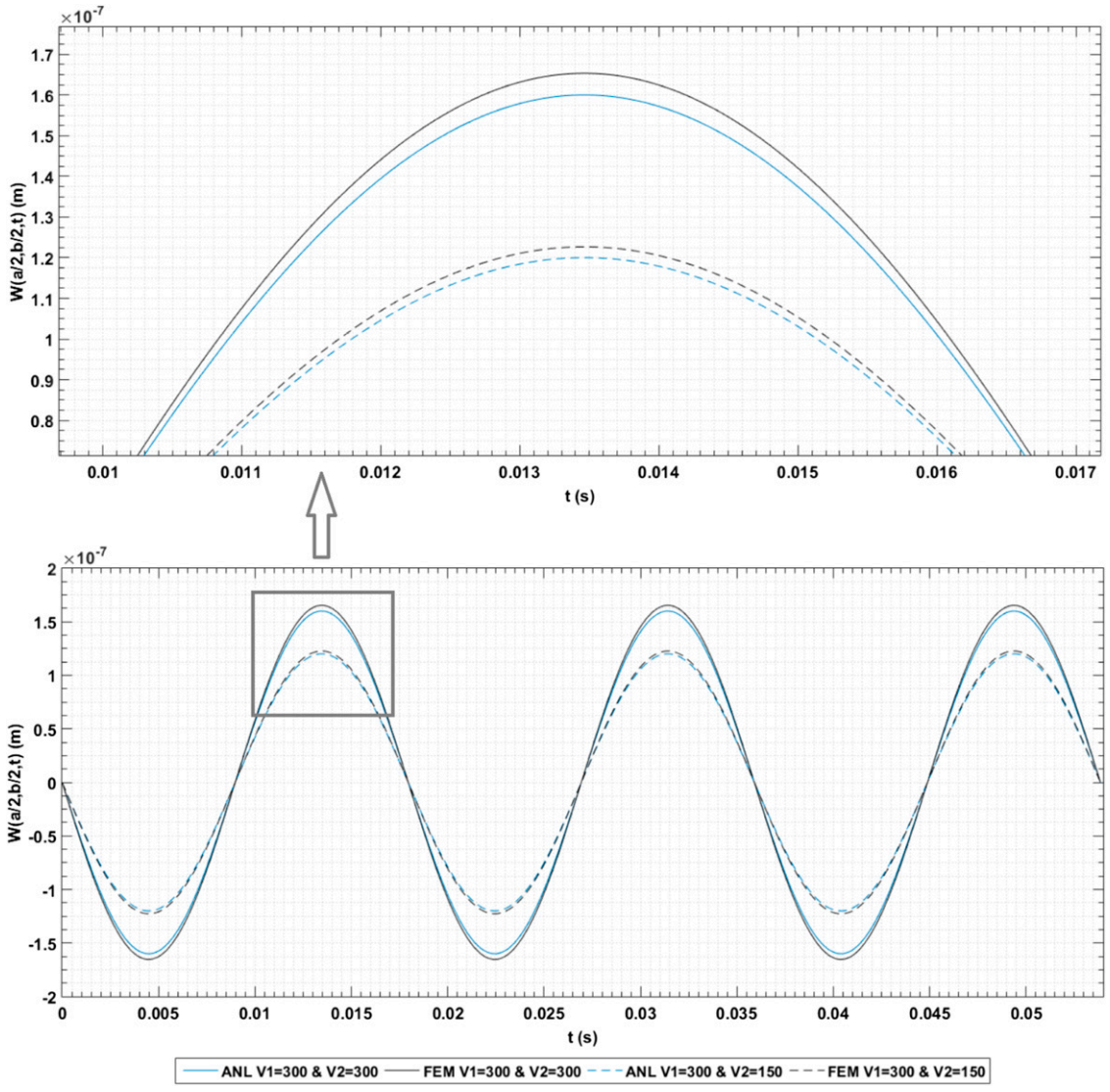

Figure 15. Vibration displacements curves at the center ($x = a/2$ (m) and $y = b/2$ (m)) of a smart laminated composite rectangular plate induced by two pairs of inclined piezoelectric actuators excited under the excitation frequency of $\phi = 350$ (rad/s) and various input voltages based on the developed analytical solution and Abaqus FEA.

$\theta \neq 0°$. As such, to evaluate twisting deformation response of laminate composite plates caused by inclination angle of piezoelectric actuators, a set of robust and realistic numerical analysis using Abaqus FEA was conducted. By comparing the analytically-determined results with the ones obtained from optimally-converged FEA, the proposed analytical solution procedure demonstrated to be able to reasonably predict twisting response of smart laminated composite plates under static or dynamic loads.

The constant electrical voltage was applied to a pair or double pairs of bonded piezoelectric actuators polarized along their thicknesses (the z direction) for static deformation response analysis. The analytical and numerical results demonstrated that inclination angle effect on static deformation response is insignificant. For dynamic deformation response analysis, the time-dependent electrical voltage was applied to one or double pairs of bonded piezoelectric actuators excited under various frequencies. The developed analytical results demonstrated that the number of piezoelectric actuators, inclination angle, excitation frequencies, and electrical voltage could all significantly impact dynamic deformation response of laminated composite plates induced by inclined piezoelectric actuators.

Although the accuracy and reliability of the proposed analytical solution was demonstrated in this study through results comparison with the numerical investigation and

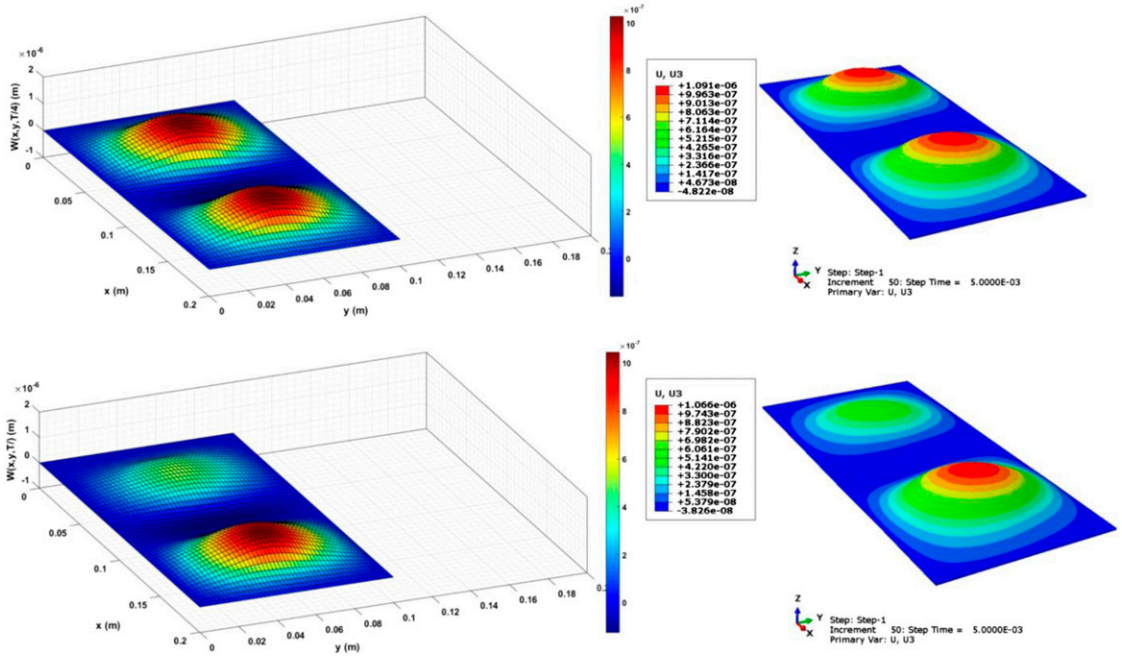

Figure 16. Laminated composite plate's mode shape with maximum amplitude based on the developed analytical solution (left) and optimally-converged FEA (right). In the first case (top), both pairs of inclined piezoelectric actuators are subjected to the voltage of 300 (V) and in the second case (bottom), the first pairs and the second pairs of inclined piezoelectric actuators are subjected to the voltages of 300 (V) and 150 (V), respectively.

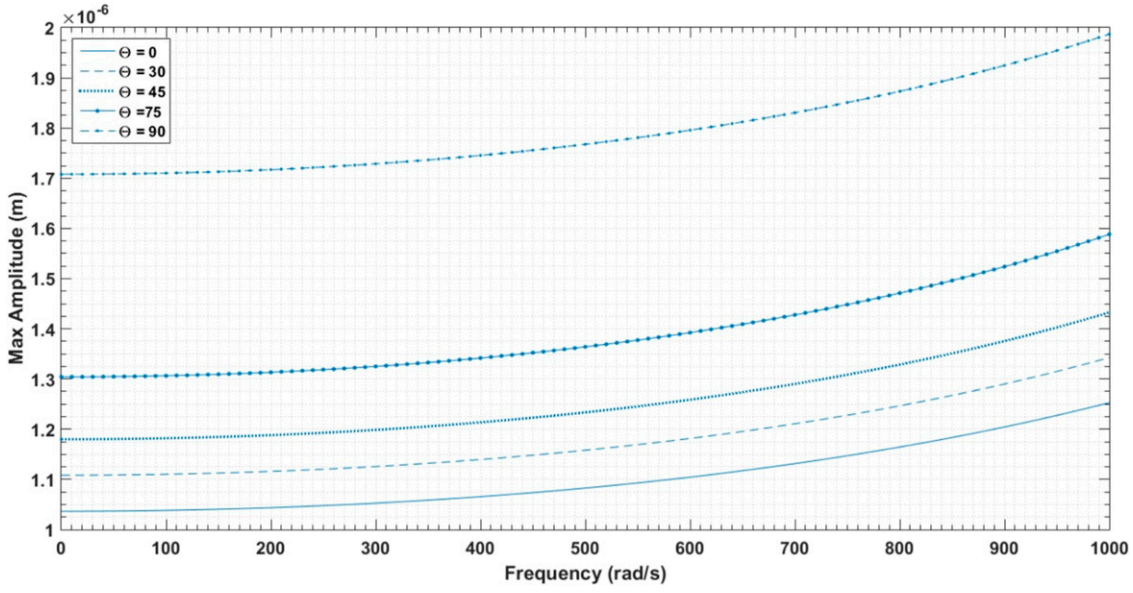

Figure 17. Correlation between maximum amplitude of vibration, inclination angle of inclined piezoelectric actuators, and the excitation frequency within a finite range of ϕ = [0–1000] (rad/s).

published literature, a comprehensive experimental study is still required in order to comprehend such phenomena in the real world. As such, the future study will intend to experimentally investigate the effect of inclination angle on static and dynamic deformation response of smart laminated composite plates induced by inclined piezoelectric actuators.

Acknowledgement

The authors would like to thank the reviewers for their thoughtful comments and efforts towards improving this research paper.

Declaration of conflicting interests

The author(s) declared no potential conflicts of interest with respect to the research, authorship, and/or publication of this article.

Funding

The author(s) received no financial support for the research, authorship, and/or publication of this article.

ORCID iDs

Soheil Gohari https://orcid.org/0000-0002-2165-448X
Farzin Mozafari https://orcid.org/0000-0001-8218-4410
Reza Alebrahim https://orcid.org/0000-0002-2036-9775

References

1. Pamnani G, Bhattacharya S and Sanyal S. Analysis of interface crack in piezoelectric materials using extended finite element method. *Mech Adv Mater Struct* 2019; 26(17): 1447–1457.
2. Frecker MI. Systems and structures recent advances in optimization of smart. *J Intell MaterialJ. Intell. Mater. Syst. Struct* 2003; 14: 207–216.
3. Tzou HS, Lee HJ and Arnold SM. Smart materials, precision sensors/actuators, smart structures, and structronic systems. *Mech Adv Mater Struct* 2004; 11(4–5): 367–393.
4. Chopra I. Review of state-of-art of smart structures and integrated systems. 19th AIAA Appl Aerodyn Conf.
5. Gohari S, Golshan a, Mostakhdemin M, et al. Failure Strength of Thin-walled Cylindrical GFRP Composite Shell against Static Internal and External Pressure for various Volumetric Fiber Fraction. *Int J Appl Phys Math* 2012; 2(2): 111–116.
6. Cook AC and Vel SS. Multiscale analysis of laminated plates with integrated piezoelectric fiber composite actuators. *Compos Struct* 2012; 94(2): 322–336.
7. Lin CC, Hsu CY and Huang HN. Finite element analysis on deflection control of plates with piezoelectric actuators. *Compos Struct* 1996; 35(4): 423–433.
8. Tahani M and Nosier A. Free edge stress analysis of general cross-ply composite laminates under extension and thermal loading. *Compos Struct* 2003; 60(1): 91–103.
9. Yang SM and Bian JJ. Vibration suppression experiments on composite laminated plates using an embedded piezoelectric sensor and actuator. *Smart Mater Struct* 1996; 5(4): 501–507.
10. Thinh TI and Ngoc LK. Static behavior and vibration control of piezoelectric cantilever composite plates and comparison with experiments. *Comput Mater Sci* 2010; 49(4 Suppl L): S276–S280.
11. Chung NT, Thuy NN, Thu DTN, et al. Numerical and experimental analysis of the dynamic behavior of piezoelectric stiffened composite plates subjected to airflow. *Math Probl Eng.Figure* 2019; 1: 2019.
12. Lam KY, Peng XQ, Liu GR, et al. A finite-element model for piezoelectric composite laminates. *Smart Mater Struct* 1997; 6(5): 583–591.
13. Balamurugan V and Narayanan S. Shell finite element for smart piezoelectric composite plate/shell structures and its application to the study of active vibration control. *Finite Elem Anal Des* 2001; 37(9): 713–738.
14. Alimohammadi H and Izadi Babokani B. Finite element electrodynamics modeling of a layered piezoelectric composite shell with different materials by using numerical software. *ISSS J Micro Smart Syst* 2020; 9(1): 79–88.
15. Lammering R and Mesecke-Rischmann S. Multi-field variational formulations and related finite elements for piezoelectric shells. *Smart Mater Struct* 2003; 12(6): 904–913.
16. Carrera E, Boscolo M and Robaldo A. Hierarchic multilayered plate elements for coupled multifield problems of piezoelectric adaptive structures: formulation and numerical assessment. *Arch Comput Methods Eng* 2007; 14(4): 383–430.
17. Zboinski G. *Problems of hierarchical modelling and hp-adaptive finite element analysis in elasticity, dielectricity and piezoelectricity.* Perusal Finite Elem. Method, 2016, pp. 1–30.
18. Picchio V, Cammisotto V, Pagano F, et al. *We are IntechOpen , the world ' s leading publisher of Open Access books Built by scientists , for scientists TOP 1 %.* IntechopenIntechopen, 2018, pp. 157–192.
19. Askari Farsangi MA and Saidi AR. Levy type solution for free vibration analysis of functionally graded rectangular plates with piezoelectric layers. *Smart Mater Struct* 2012; 21(9).
20. Askari Farsangi MA, Saidi AR and Batra RC. Analytical solution for free vibrations of moderately thick hybrid piezoelectric laminated plates. *J Sound Vib* 2013; 332(22): 5981–5998.
21. Kapuria S, Dube GP, Dumir PC, et al. Levy-type piezothermoelastic solution for hybrid plate by using first-order shear deformation theory. *Compos B Eng* 1997; 28(5–6): 535–546.
22. Vel SS and Batra RC. Exact solution for the cylindrical bending of laminated plates with embedded piezoelectric shear actuators. *Smart Mater Struct* 2001; 10(2): 240–251.
23. Gohari S, Sharifi S and Vrcelj Z. New explicit solution for static shape control of smart laminated cantilever piezo-composite-hybrid plates/beams under thermo-electro-mechanical loads using piezoelectric actuators. *Compos Struct* 2016; 145: 89–112.
24. Sobhy M. Levy solution for bending response of FG carbon nanotube reinforced plates under uniform, linear, sinusoidal and exponential distributed loadings. *Eng Struct* 2019; 182: 198–212.
25. Gohari S, Sharifi S and Vrcelj Z. A novel explicit solution for twisting control of smart laminated cantilever composite plates/beams using inclined piezoelectric actuators. *Compos Struct* 2017; 161: 477–504.

26. Abaqus and Systemes Dassault. *Abaqus FEA software*, 2018.
27. Wang H, Li Z and Zheng S. Size-dependent deflection of cross-ply composite laminated plate induced by piezoelectric actuators based on a re-modified couple stress theory. *Arch Mech* 2019; 71(3): 177–205.
28. Shao D, Hu F, Wang Q, et al. Transient response analysis of cross-ply composite laminated rectangular plates with general boundary restraints by the method of reverberation ray matrix. *Compos Struct* 2016; 152: 168–182.
29. Her S-C and Lin C-S. Vibration analysis of composite laminate plate excited by piezoelectric actuators. *Sensors* 2013; 13: 2997–3013.
30. Shaik Dawood MSI, Iannucci L and Greenhalgh ES. Three-dimensional static shape control analysis of composite plates using distributed piezoelectric actuators. *Smart Mater Struct* 2008; 17(2): 1–10.
31. Tamijani AY, Abouhamze M, Mirzaeifar R, et al. Feedback control of piezo-laminate composite plate. 14th International Congress on sounds and VibrationCairns Australia, 2007: 12.

Appendix

Nomenclature

x, y, z	A Cartesian coordinate system for a three-dimensional space
a	Length of rectangular plate
b	Width of rectangular plate
t_p	Piezoelectric thickness
h	Distance between the top or bottom surfaces of layer k and the centroid of the rectangular cross-section
H	Total thickness of composite plate
k	Layer number
N	Total number of layers
L	Total number of pairs of piezoelectric actuators
t	Time
V	Electrical voltage
ρ_z	Electrical permittivity
d_{31}, d_{32}	Piezoelectric coefficients
$W(x,y)$	Lateral (transverse) displacement along the z axis
$P^e(x, y)$	Expression for electrical bending and twisting couplings
ρ	Density of composite plate
ϕ	Piezoelectric excitation frequency
Ψ_z	Total electrical potential applied to a piezoelectric actuator
θ	Inclination angle between a piezoelectric actuator and the x axis
x_1, x_2, y_1, y_2	Placement of piezoelectric actuators on the xy plane
E_1, E_2	Elasticity modulus in a composite material in the fiber and transverse directions, respectively
G_{12}	In-plane shear modulus in a composite material
v_{12}	In-plane Passion's ratio in a composite material
D_{ij}	Flexural rigidity of a composite material
Q_{ij}	Elements of the stiffness matrix in a composite plate
$\overline{Q}_{ij}$	Elements of the reduced stiffness matrix in a composite plate
$\overline{H}$	Unit step function
δ	Delta/shooting function
$M_x(x,y)$	Mechanical bending moment about the x axis
$M_y(x,y)$	Mechanical bending moment about the y axis
$M_{xy}(x,y)$	Mechanical twist in the xy plane
$M_x^e(x,y)$	Electrical bending moment about the x axis
$M_y^e(x,y)$	Electrical bending moment about the y axis
$M_{xy}^e(x,y)$	Electrical twist in the xy plane
w_{mn}	Higher-order finite integral transform of the mid-plane lateral displacement
α_m, β_n	Angular terms used in the Fourier series